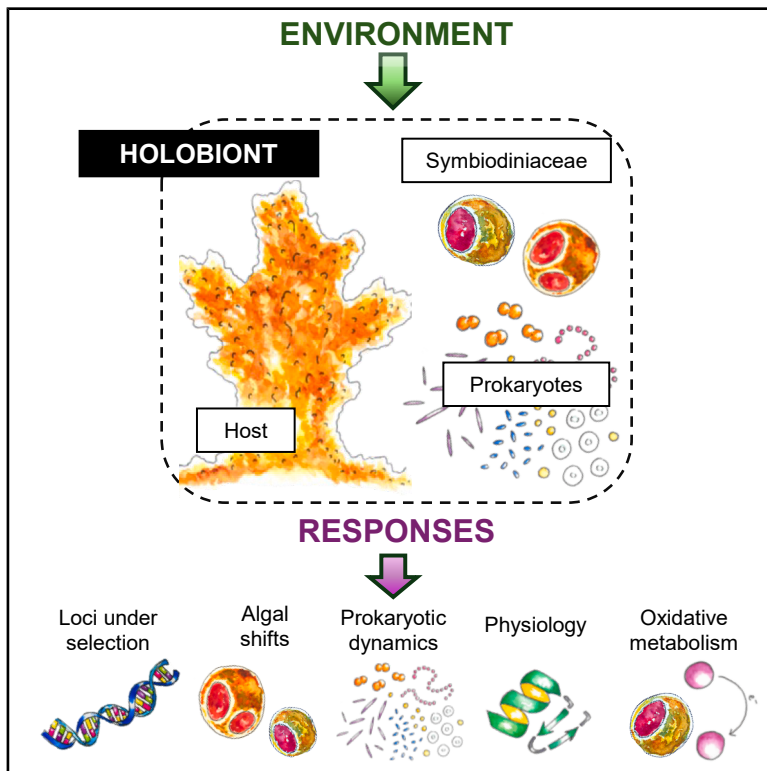


Current Biology

The role of holobiont composition and environmental history in thermotolerance of Tropical Eastern Pacific corals

Graphical abstract



Authors

Victoria M. Glynn,
 Laura Fernandes de Barros Marangoni,
 Maxime Guglielmetti, ...,
 Matthieu Leray, Sean R. Connolly,
 Rowan D.H. Barrett

Correspondence

connollys@si.edu (S.R.C.),
 rowan.barrett@mcgill.ca (R.D.H.B.),
 victoria.glynn@mail.mcgill.ca (V.M.G.)

In brief

Glynn et al. investigate coral-microbiome interactions under thermal stress in Panama's Tropical Eastern Pacific, finding that regional environmental regimes, host lineage, and algal microbiomes influence *Pocillopora* coral thermotolerance. This study provides an integrated view of the mechanisms underlying differences in coral bleaching.

Highlights

- Seasonal changes shape selection on genes implicated in thermotolerance
- Thermal stress drives contrasting algal and prokaryotic microbiome dynamics
- Region and host lineage shape physiological and oxidative responses to heat stress

Article

The role of holobiont composition and environmental history in thermotolerance of Tropical Eastern Pacific corals

Victoria M. Glynn,^{1,2,8,12,*} Laura Fernandes de Barros Marangoni,² Maxime Guglielmetti,^{3,9,10} Eunice R. Tapia,^{2,4} Viviane Ali,² Helio Quintero,² E. Catalina Rodriguez Guerra,² Matan Yuval,⁵ David I. Kline,^{2,6} Matthieu Leray,^{2,11} Sean R. Connolly,^{2,7,11,*} and Rowan D.H. Barrett^{1,11,*}

¹Department of Biology and Redpath Museum, McGill University, Montréal, QC H3A 1B1, Canada

²Naos Marine Laboratories, Smithsonian Tropical Research Institute (STRI), Ancón, Panamá, Republic of Panama

³Department of Biology, McGill University, Montréal, QC H3A 1B1, Canada

⁴Facultad de Ciencias Naturales, Exactas y Tecnología, University of Panama, Vía Simón Bolívar, Panamá, Republic of Panama

⁵School of Marine Sciences, University of Haifa, Haifa 3498838, Israel

⁶Scripps Institution of Oceanography, University of California San Diego, La Jolla, San Diego, CA 92037, USA

⁷College of Science and Engineering, James Cook University, Townsville, QLD 4811, Australia

⁸Present address: Department of Biology, University of Vermont, 109 Carrigan Drive, Burlington, VT 05405, USA

⁹Present address: Institut de recherche en biologie végétale, Département de sciences biologiques, Université de Montréal, 4101 Sherbrooke Est, Montréal, QC H1X 2B2, Canada

¹⁰Present address: Département des Sciences Biologiques, Université de Montréal, 1375 Avenue Thérèse-Lavoie-Roux, Montréal, QC H2V 0B3, Canada

¹¹Senior author

¹²Lead contact

*Correspondence: victoria.glynn@mail.mcgill.ca (V.M.G.), connollys@si.edu (S.R.C.), rowan.barrett@mcgill.ca (R.D.H.B.)
<https://doi.org/10.1016/j.cub.2025.05.035>

SUMMARY

Coral reefs support approximately 25% of all marine life, making it essential to understand the factors impacting their ability to withstand climate change. Corals' response mechanisms encompass both the host's own potential and that of a diverse microbial community, collectively known as the holobiont. Research investigating how these co-evolved taxa affect each other during thermal stress has revealed both the vulnerability and resilience of coral reefs, but the precise mechanisms underlying different bleaching trajectories are still poorly understood. We implemented a standardized acute thermal stress assay to investigate how seasonal upwelling in Panama's Tropical Eastern Pacific (TEP) influences *Pocillopora* coral's host-microbiome configurations, and we tested holobionts' resistance to increasing temperatures. Despite little host genetic differentiation, algal community shifts were modulated by both region and genetic lineage. This pattern strongly contrasted with temperature-driven dysbiosis for the prokaryotic community. Host stress responses differed among regions during acute thermal stress. Regional variation in total antioxidant capacity suggested that corals from the region with seasonal upwelling experience more stressful baseline conditions, which may contribute to their higher predicted thermal thresholds as estimated via host protein concentrations. Furthermore, shifts in algal microbiomes were associated with changes in host thermotolerance, as captured by host physiology and oxidative metabolism, suggesting a possible link between microbiome composition and host physiological performance. By leveraging the natural laboratory created by Panama's TEP, we demonstrate that coral holobionts from nearby gulfs with different thermal dynamics differ in their ability to withstand thermal stress, providing new insights into the factors driving coral thermotolerance.

INTRODUCTION

Understanding the mechanisms underlying organismal responses to environmental stress has been a long-standing pursuit in evolutionary biology, but anthropogenic climate change has made this interest an imperative. Most prior research on species persistence under climate change has investigated the ability of single taxa to respond to environmental stress via acclimation or adaptation, emphasizing how standing genetic variation

and phenotypic plasticity together shape the evolutionary potential of organisms.^{1–5} There is increasing evidence that species interactions such as facilitation, competition, and predation can modulate how individual taxa respond to environmental stress.^{6–9} Interactions that can have reciprocal impacts on the development, fitness, and evolution of multiple species are those occurring between a host and its microbiome (i.e., bacteria, archaea, microbial eukaryotes, and viruses), collectively known as the holobiont.^{10–12} Compared with a host- or microbe-centric

view, a holobiont approach allows us to consider how different host-microbiome configurations are shaped by and in turn respond to their environmental context. Although the importance of host-microbiome interactions for organismal health and functioning is well recognized,^{13–15} few studies have simultaneously measured responses in the host as well as both prokaryotic and algal components of microbiomes.^{16–18}

Corals are a model system to explore the consequences of climate change on host-microbiome interactions because they associate with a highly diverse microbial community that has been implicated in their resilience to thermal stress.^{19–22} Coral bleaching is a biological process in which environmental stressors disrupt the coral-algae symbiosis. As a result, corals become pale due to the loss of the algal symbionts residing within their tissues.^{23,24} Some of these algal symbionts, which belong to the family Symbiodiniaceae, have been linked to differences in coral's thermal tolerance. For instance, in the Gulf of Chiriquí in Panama's Tropical Eastern Pacific (TEP), differences in thermotolerance have been associated with a switch from *Cladocopium* spp. to *Durusdinium* spp., with *Durusdinium* spp.-dominated colonies shown to be most thermally tolerant during both El Niño events and predicted to best persist under future warming scenarios.^{25,26} Besides Symbiodiniaceae, bacterial, viral, and archaeal communities can also vary in response to stress and have been shown to influence coral health, particularly within the context of disease, as the presence of certain microorganisms has been linked to coral tissue loss and subsequent mortality.^{27–31} Inoculating corals with prokaryotic cultures that have specific genetic and/or phenotypic characteristics can reduce bleaching and pathogen presence, further underscoring the microbiome's importance in coral health.^{32,33} Although there is a large body of work on microbial dynamics during bleaching, few studies simultaneously track physiological responses for the host,^{17,18} making it difficult to gauge potential interactions between host and microbiome response mechanisms.

Independent of its microbiome, the coral host can respond to increasing temperatures via both genetic adaptation and physiological plasticity. A hallmark of bleaching involves photoinhibition and damage to the algal chloroplast that results in an accumulation of reactive oxygen species (ROS), and an increase in ROS in turn damages both algal and coral host tissues.^{23,24,34–36} The balance between oxidative metabolism (e.g., ROS-triggered oxidative damage and total antioxidant capacity [TAC]) and physiological bleaching responses (e.g., chlorophyll *a* and host protein content) during thermal stress has been linked to coral's baseline stress levels and their ability to offset the impacts of environmental stress,^{37–41} although the hypothesis that ROS plays a causal role in bleaching has also been challenged.^{42–45} In addition to these metabolically driven intracellular processes, fast-acting genetic mechanisms such as transcriptional plasticity have emerged as a key acclimation response, where more resilient corals have a higher basal expression of key genes involved in processes such as protein folding and innate immune response prior to thermal stress.^{46–48} Recent evidence further suggests that algal symbionts modulate gene expression patterns in the host, resulting in different bleaching outcomes.^{49,50} Finally, variation in coral thermal tolerance has been shown to be a heritable polygenic trait, implying that longer-term evolutionary responses might be possible if genetically based trait

changes can keep pace with the rate of environmental change.^{51–57} It is currently unclear how this diverse suite of host response mechanisms interacts with microbial dynamics to yield divergent bleaching responses.

Insights about coral bleaching response mechanisms have predominantly emerged from a combination of correlative analyses of natural populations during bleaching events^{58–60} and long-term thermal stress experiments on the order of weeks to months.^{61–63} Although these studies have provided foundational data on the drivers of coral bleaching resistance, the mechanisms underlying different bleaching trajectories are still poorly understood because the diversity of experimental approaches employed makes drawing inferences between studies a challenge. Standardized short-term assays offer a portable and cost-effective solution to this issue by facilitating comparisons of estimated thermal thresholds between regions, populations, and taxa. These assays also facilitate the exploration of various coral stress response mechanisms simultaneously, from microbiome dynamics to oxidative metabolism, improving our understanding of the mechanistic links within the coral holobiont and, in turn, their consequences for thermotolerance.^{64–66}

Panama's TEP has long served as a natural laboratory to explore the factors driving coral holobiont's responses to climate change,^{67–69} and represents an ideal location for coral thermotolerance studies employing standardized short-term assays. Across Panama's TEP, *Pocillopora* corals form the foundation of the reef framework.^{70,71} Corals from this genus experience strong, upwelling-mediated, intra-annual environmental variability in the Gulf of Panama, whereas they experience weak upwelling in the Gulf of Chiriquí. Upwelling is the process by which cold, nutrient-rich water displaces warmer, less nutrient-rich surface water. In the Gulf of Panama (and to a much lesser degree in the Gulf of Chiriquí), upwelling drives large annual fluctuations in temperature, pH, oxygen, and nutrients.^{72–74} There is considerable debate about whether the abiotic heterogeneity triggered by upwelling may influence the physiological and microbial mechanisms underlying differences in bleaching resilience.^{75–80} With only one study to date exploring these reef's experimental responses to thermal stress,⁶¹ complementing observational data with a standardized acute thermal assay in Panama's TEP has the potential to further illuminate how host and microbiome stress response mechanisms are shaped by the region's upwelling regime and together are driving different bleaching trajectories, and how these compare with how corals in other reef regions respond to comparable thermal stress.

In this study we test how the different environmental regimes of the Gulfs of Panama and Chiriquí in Panama's TEP have shaped thermotolerance mechanisms for the coral holobiont. In leveraging an acute thermal stress assay known as the coral bleaching automated stress system (CBASS; following Voolstra et al.⁶⁴), we present a comprehensive view of the holobiont's thermotolerance pathways by incorporating host genetics, algal and prokaryotic community dynamics, and host physiological and oxidative metabolism data. In coral hosts, we hypothesized that we would detect a signature of local adaptation to each gulf due to the differences in mean and interannual variability in temperature primarily driven by upwelling. This would be manifested through loci associated with thermal stress responses showing exceptional genetic differentiation relative to the rest of the

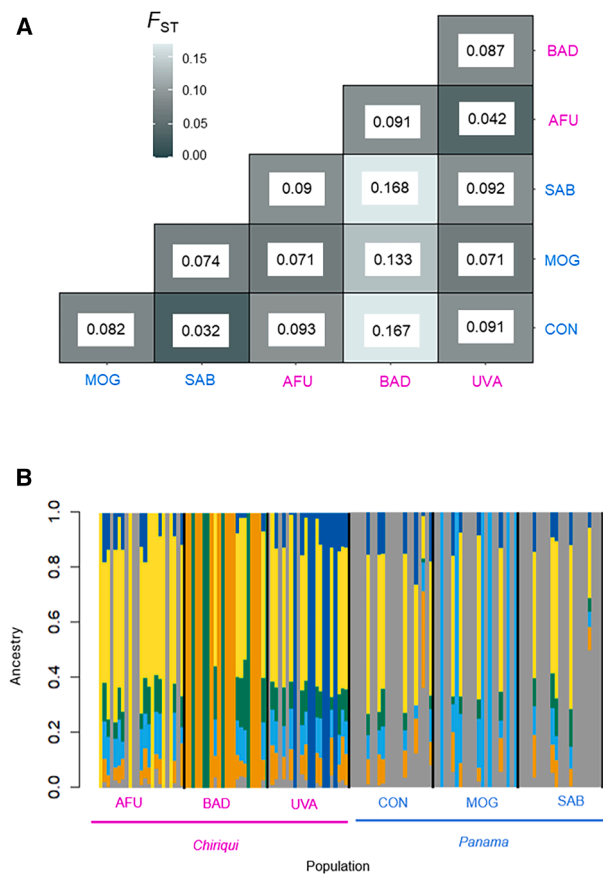


Figure 1. Population genetics of *Pocillopora* corals across Panama's TEP

Each reef site is denoted by its three-letter code. AFU, Canal de Afuera; BAD, Bahía Damas; UVA, Uvas; CON, Contadora; MOG, Mogo Mogo; SAB, Saboga. (A) Pairwise fixation index (F_{ST}) values among the 137 *Pocillopora* coral colonies across six reefs in Panama's Tropical Eastern Pacific (TEP). F_{ST} calculations here are based on Weir and Cockerham's estimate (1984).

(B) Ancestral populations across Panama's TEP as detected via ADMIXTURE.⁸² A total of six ancestral populations were identified, corresponding to six reefs across two different regions. Each line on the plot represents a single individual, where the colors within represent the different identified ancestral populations. Thick black lines delineate different reefs, which are further separated and color-coded by region, Gulf of Chiriquí and Gulf of Panama, respectively. See [Data S1A](#) for additional population genetic metrics. See also [Figure S1](#).

genome. Because *Durusdinium* spp. has previously been associated with more thermotolerant *Pocillopora* corals in the TEP,^{25,26} we hypothesized that the most thermally resistant colonies would be dominated by *Durusdinium* spp. We also predicted that corals from the Gulf of Panama, which are exposed to a more seasonally variable environment, would experience less microbial dysbiosis during thermal stress. This should manifest via lower among-colony variance in community composition at higher temperatures, which is in line with the Anna Karenina principle (AKP) (see Zaneveld et al.⁸¹), which argues that increased microbiome dispersion is indicative of greater host stress. Furthermore, we also hypothesized that, in high-temperature treatments, corals from the Gulf of Panama would have

higher predicted thermal thresholds on the basis of host protein and chlorophyll a content and a more effective biochemical apparatus to scavenge and neutralize ROS compared with corals from the Gulf of Chiriquí. This is presumably due to the greater temperature variability in the Gulf of Panama (see O'Dea et al.⁷³). By experimentally testing the responses of different holobiont configurations driven by upwelling, we aim to increase our understanding of the complex mechanisms by which the host and microbiome interact to govern corals' responses to environmental change.

RESULTS

Signatures of local adaptation to upwelling amidst high gene flow

Our population genetic analyses indicated that although there is negligible genetic differentiation across the two gulfs in Panama's TEP, there are signatures of potential local adaptation to each gulf's upwelling regimes. We found a mean F_{ST} value of 0.0333 between gulfs, indicating a high degree of gene flow between locations ([Data S1A](#); [Figure 1A](#)). This lack of genetic differentiation was further supported by our ADMIXTURE analysis, as all six ancestral populations are found within each gulf, suggesting a high degree of admixture across our study sites ([Figure 1B](#); [Figure S1](#)). When running the above analyses per mitochondrial open reading frame (mtORF) lineage, here mtORF 1 (*P. grandis*/*P. meandrina*) and mtORF 3 (*P. cf. verrucosa*), and additionally running *pcadapt* to detect signatures of local adaptation, we found that the majority of between-gulf gene flow appears to be occurring within mtORFs ([Figure S2](#)). However, a between-mtORF F_{ST} value of 0.1697 and the mixed ancestry of many individuals suggest that the two mtORFs are not completely isolated lineages ([Figures S1](#) and [S2](#); [Data S1A](#)).

Given the lack of evidence for strong genetic differentiation across mtORFs, we detected putative outlier loci for both lineages together across gulfs. Consistent with our hypothesis, we found evidence for strong differentiation in a small number of outlier loci. Between-gulf comparisons using the F_{ST} -based approach, OutFLANK detected 11 outlier loci at a q -value cutoff of 0.05 and expected heterozygosity cutoff of 0.1 ([Figure 2](#); full list of loci can be found in [Data S1B](#)). Analysis with *snpeff* revealed that two of these loci have a predicted impact on protein-coding regions, corresponding to a missense and intron variant, respectively. These variants are located in a predicted Rab-20-like protein (missense variant) and a predicted hemicen-tin-2-like protein (intron variant; [Data S1B](#)).

Shifts in Symbiodiniaceae community composition during the CBASS

Over the course of the CBASS, we observed marked differences across regions and mtORFs in the relative abundance of different Symbiodiniaceae internal transcribed spacer 2 (ITS2) type profiles ([Figure 3](#)). However, we did not observe colonies at 36°C having the highest relative prevalence of *Durusdinium* spp. type profiles, as we had initially hypothesized. Instead, when comparing mtORFs, we found that mtORF 1 colonies were dominated by *Durusdinium* spp. type profiles, with an increase in the relative prevalence of *Cladocopium* spp. type profiles at 36°C. By contrast, *Cladocopium* spp. type profiles were dominant

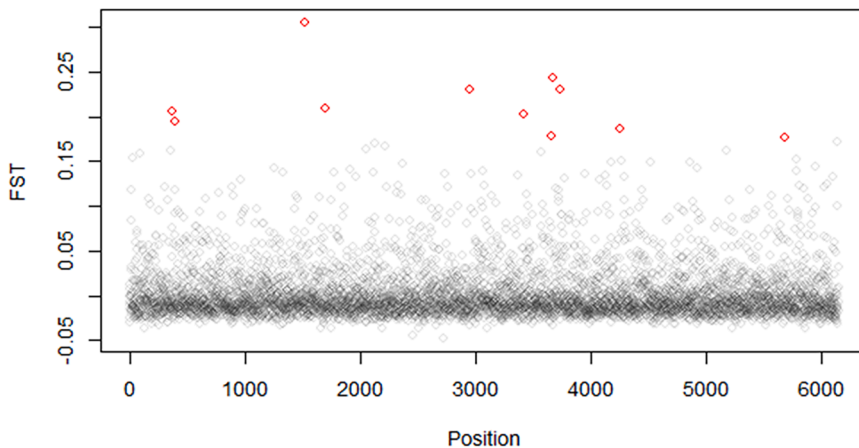


Figure 2. Loci under putative selection (outlier SNPs) across coral samples from Panama's TEP

Each point denotes a locus, with genomic position (x axis) plotted against F_{st} (y axis). Loci in red are considered outlier SNPs based on a q-value cutoff of 0.05 and an expected heterozygosity cutoff of 0.1. See [Data S1B](#) for a full characterization of detected outlier SNPs.

across the temperature treatments for mtORF 3 colonies. These trends were supported by our generalized least squares (GLS) model, which detected two separate, significant interactions: (1) between temperature and region and (2) between temperature and mtORF, which explained differences in the relative abundance of *Cladocopium* spp. versus *Durusdinium* spp. defining intragenomic (ITS2 sequence) variants (DIVs) ([Data S1C](#)). Although we observed inter-colony variability in algal shifts, these recapitulate the trends observed at the treatment level for mtORF 1 colonies ([Figure S3A](#)). For mtORF 3, we observe that many colonies from the Gulf of Panama have *Cladocopium* spp. ITS2 type profiles dominant even at 36°C, with the few colonies increasing their relative proportions of *Durusdinium* type profiles doing so seemingly randomly with respect to temperature ([Figure S3B](#); see [Figure S4](#) for a breakdown of the distribution of mtORF lineages across sampling sites). Note that we did not analyze microbiomes at temperatures above 36°C because tissue sloughing was visually apparent at temperature treatments above this level.

When considering Symbiodiniaceae community composition shifts throughout the CBASS, our canonical analysis of principal coordinates (CAP) analysis shows a clear difference between the 36°C treatment and the three other temperature treatments. This difference is most stark for mtORF 1 colonies in the Gulf of Chiriquí ([Figure 4A](#)). Observed differences in community composition were statistically significant ($p < 0.05$) across temperatures, regions, mtORFs, and the interaction between temperature and mtORF when performing permutational multivariate analysis of variances (PERMANOVAs) ([Data S1D](#)). Comparison of effect sizes on the basis of the pseudo-F-statistic revealed that mtORF was the strongest driver of Symbiodiniaceae communities across all statistically significant factors, followed by region ([Data S1D](#)). Pairwise post-hoc analyses revealed that Symbiodiniaceae communities were distinct when comparing the highest temperature treatment, here 36°C, with 28.5°C and 33°C ([Data S1E](#)). We also detected significant differences in variance across temperature treatments, yet these results were contrary to our expectations. Post-hoc tests revealed that samples at 36°C were less variable as compared with all other temperature treatments, indicative of less microbial dysbiosis at the highest temperature treatment ([Figure S5A](#); [Data S1F](#)), which is contrary to our predictions per the AKP (see Zaneveld et al.⁸¹).

When considering each region and mtORF combination separately (e.g., mtORF 1 from the Gulf of Panama), indicator species analyses revealed 23 taxa that were differentially associated with mtORF 1 from the Gulf of Chiriquí. All but one taxon was associated with the highest temperature treatment of 36°C, and all of these correspond to various *Cladocopium* spp. taxa. The only taxon not associated with 36°C was uniquely associated with the remaining three temperature treatments and was identified as being *Durusdinium* spp. ([Data S1G](#)).

Temperature-induced microbial dysbiosis occurs during the CBASS

Analysis of the prokaryotic microbiome revealed notable shifts in community composition between the baseline and the highest temperature treatment. Given the higher taxonomic diversity of the prokaryotic community as compared with the Symbiodiniaceae community, we focused on aggregate community differences across amplicon sequence variants (ASVs) as measured by statistics such as Bray-Curtis dissimilarity, rather than shifts in particular taxa. These community differences were visualized using ordination plots, as our goal was to explore patterns of community similarity and the factors potentially driving observed groups. Our CAP analyses showed an increase in dispersion at the 36°C treatment as compared with the other three temperature treatments, as we had hypothesized, yet this pattern was seen across all region-mtORF groupings ([Figure 4B](#)). Community dissimilarity trends were only statistically significant ($p < 0.05$) across regions, with differences across temperatures and the interaction between temperature and region, temperature and mtORF, region and mtORF, and the three-way interaction between temperature, region, and mtORF emerging as non-significant ([Data S1H](#)). In testing for differences in homogeneity of variance, we detected significant differences across temperature treatments, with post-hoc tests revealing that this was driven by samples at 36°C being more variable as compared with all other temperature treatments ([Figure S5B](#); [Data S1I](#)), in line with the AKP (see Zaneveld et al.⁸¹). In considering each region and mtORF combination separately (e.g., mtORF 1 from the Gulf of Panama), indicator species analyses did not identify any differentially associated prokaryotic ASVs.

Physiological responses to thermal stress were mediated by region and mtORF lineage

Physiological responses during the CBASS, captured via both host protein and chlorophyll a concentrations, reveal that bleaching responses varied among regions and, in some cases,

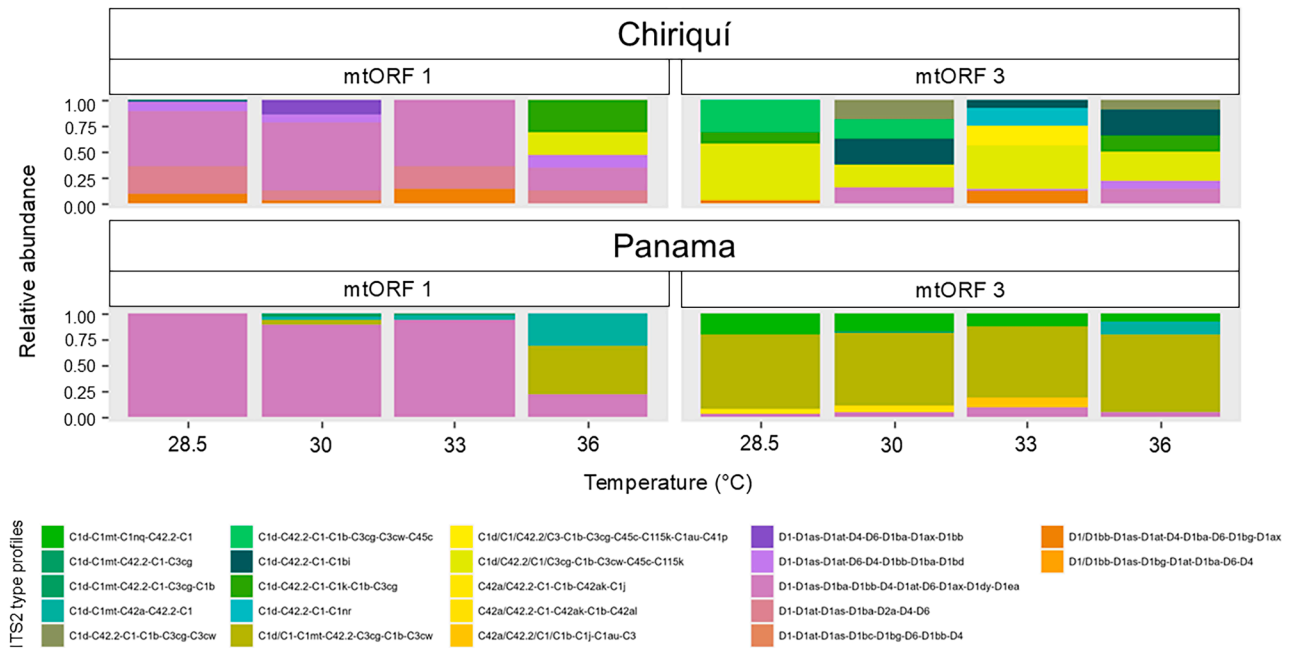


Figure 3. Changes in *Pocillopora* ITS2 type profiles during the CBASS, across regions and mtORF lineages

Relative abundances of ITS2 type profiles are shown on the x axis and temperature treatments on the y axis. DIVs starting with a “C” correspond to *Cladocopium* spp., and those starting with a “D” correspond to *Durusdinium* spp. See [Data S1C](#) for GLS modeling results for *Cladocopium* spp. and *Durusdinium* spp. DIV relative abundances. See [Figure S3](#) for individual colonies’ ITS2 type profiles. See also [Figure S4](#).

mtORF lineages. For host protein concentrations during the CBASS, our best-fitting non-linear model included a fixed effect of region for the 50% temperature threshold (α_T) and threshold steepness (δ_T), such that the protein content of corals in the Gulf of Panama was maintained at near-ambient levels under higher temperature conditions as compared with corals from the Gulf of Chiriquí, consistent with our hypothesis that corals in the Gulf of Panama would be more thermotolerant ([Figure 5A](#); [Data S2A](#)). Random site-level variation in the maximum protein concentration (ν_s) and threshold steepness (δ_s) was also present. There was no evidence for a significant effect of mtORF lineage on host protein content over the course of the experiment. The 50% temperature threshold for the corals in the Gulf of Panama was approximately 1.2°C higher than for corals in the Gulf of Chiriquí, while the threshold steepness and maximum protein concentrations were highly variable across sites ([Figure 5A](#); [Data S2B](#)).

For chlorophyll *a* concentrations during the CBASS, the best-fitting non-linear model included a fixed effect of region on the maximum chlorophyll concentration (ν_T) and a fixed effect of the interaction between region and mtORF on both the 50% temperature threshold ($\alpha_{r,m}$) and threshold steepness ($\delta_{r,m}$). This model showed that chlorophyll *a* concentrations were best maintained at near-ambient levels under high-temperature conditions for mtORF 3 colonies across gulfs ([Figure 5B](#); [Data S2C](#)). Additionally, we found evidence of site-level variation only for the threshold steepness (δ_s). During our acute thermal stress assay, maximum chlorophyll *a* concentrations in the Gulf of Chiriquí were ~37% higher than for the Gulf of Panama ([Figure 5B](#)). There was also a markedly steeper threshold for mtORF 1 corals in the

Gulf of Panama, which was also reflected in the estimated parameter values ([Figure 5B](#); [Data S2D](#)).

Levels of oxidative damage to lipids were strongly associated with region

Oxidative metabolism dynamics, captured by lipid peroxidation (LPO) and TAC, provide further evidence that regional upwelling regimes impact *Pocillopora* corals’ responses to temperature stress. During the CBASS, LPO levels decreased from high values at ambient temperature to intermediate values at higher temperatures in the Gulf of Panama, whereas LPO levels increased from low to intermediate values as temperature increased in the Gulf of Chiriquí ([Figure 5C](#)). Together, this implies that corals in the Gulf of Panama experienced higher baseline levels of stress and yet were able to better counteract oxidative damage as temperature increased, consistent with our hypothesis. This was reflected by our model selection, in which our best-fitting model only had an interaction effect between temperature treatment and region ([Data S2E](#) and [S2F](#)). However, post-hoc comparisons revealed that the two regions only significantly differed in their LPO at the baseline temperature treatment of 28.5°C, with all other within- and between-gulf comparisons across temperatures emerging as non-significant ([Figure 5C](#); [Data S2G](#)).

For TAC, our best-fitting model was a second-order function solely driven by temperature. Contrary to our predictions, there was no evidence for a significant effect of region or mtORF for TAC during the experiment. In the model selection process, it is important to note that our selected model performed similarly to a model that additionally had a term that represented the

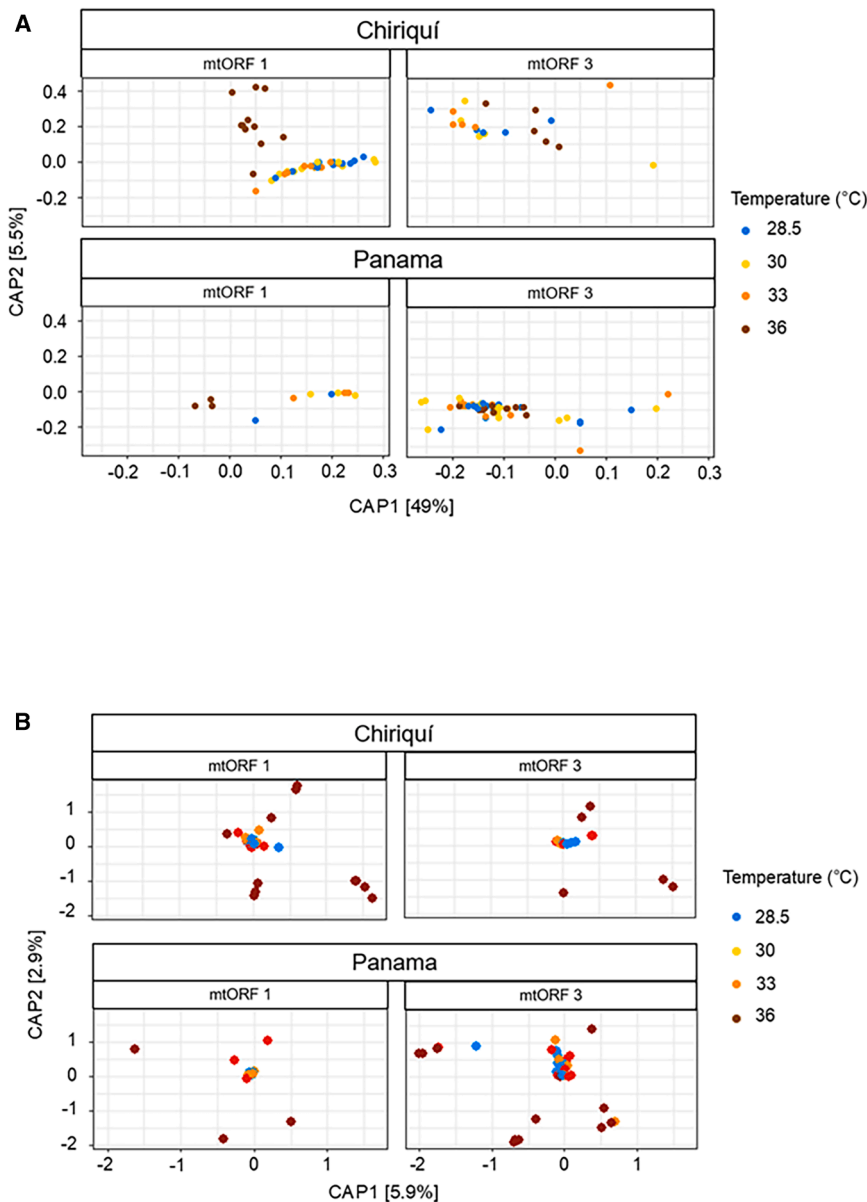


Figure 4. CAP plots for *Pocillopora* coral's microbial communities during the CBASS, based on Bray-Curtis dissimilarity in the relative abundances of DIVs for ITS2 and ASVs for 16S

(A) CAP plots for the Symbiodiniaceae communities.

(B) CAP plots for the prokaryotic communities.

See [Figure S5](#) and [Data S1D–S1I](#) for further statistical testing of the observed trends.

thermotolerance. We found evidence of divergent selection across regions on genes previously linked to coral's responses to thermal stress and differences in microbiome dynamics under thermal stress. Observational studies have documented shifts between *Cladocopium* spp. and *Durusdinium* spp. for *Pocillopora* corals in response to thermal stress in the Gulf of Chiriquí (see Palacio-Castro et al.²⁶ and Glynn et al.²⁵). By examining responses in this gulf as well as the Gulf of Panama, we additionally find that the shift to *Durusdinium* spp. is mediated by both mtORF and gulf of origin, with observed increases in *Cladocopium* spp. potentially resulting in negative fitness outcomes for the host. In contrast to the algal community shifts across temperature treatments, we observed an increase in variance for the prokaryotic community during our acute thermal stress assay, irrespective of gulf and mtORF. This is in line with previous studies on animal microbes under stress, suggesting that this component of the *Pocillopora* microbiome enters a disease-like state during our assay and that such signatures can be ascertained on shorter timescales than previously reported.^{81,83,84} In considering host

relative proportion of *Cladocopium* spp. versus *Durusdinium* spp. For the latter, as TAC increased, the relative proportion of *Durusdinium* spp. also increased. The temperature and algal shifts model marginally outperformed (1) the temperature and mtORF model and (2) the temperature and region model. However, in comparing Akaike information criterion (AIC) and log-likelihood values and in choosing the most parsimonious model, the model with only temperature was selected (see [Data S2H–S2J](#)). Predicted responses for our best-fitted model showed a clear parabolic decrease for TAC throughout the experiment as the temperature increased up to 36°C ([Figure 5D](#)).

DISCUSSION

Our study reveals a nuanced interplay of environment, host genetics, and microbiome in driving differences in coral

response pathways, across both gulfs we find that mtORF 1 colonies experience more stress than mtORF 3 colonies, but in general, corals from the Gulf of Panama experience less thermal stress during the CBASS than those from the Gulf of Chiriquí. This finding bolsters previous hypotheses positing that within the TEP, the increased temporal environmental variability caused by upwelling may produce more thermally resistant corals (see Randall et al.⁷⁷ and Rodríguez-Ruano et al.⁷⁸). It is important to note that although seasonal upwelling is a defining feature of our study sites in Panama's TEP, other environmental parameters could also influence the observed differences across gulfs, notably seawater temperature and bleaching history. Although the Gulf of Chiriquí has a higher mean temperature and, prior to our study, only the corals in this gulf had experienced mass bleaching (see Randall et al.⁷⁷), corals in the Gulf of Panama showed the most overall thermotolerance during

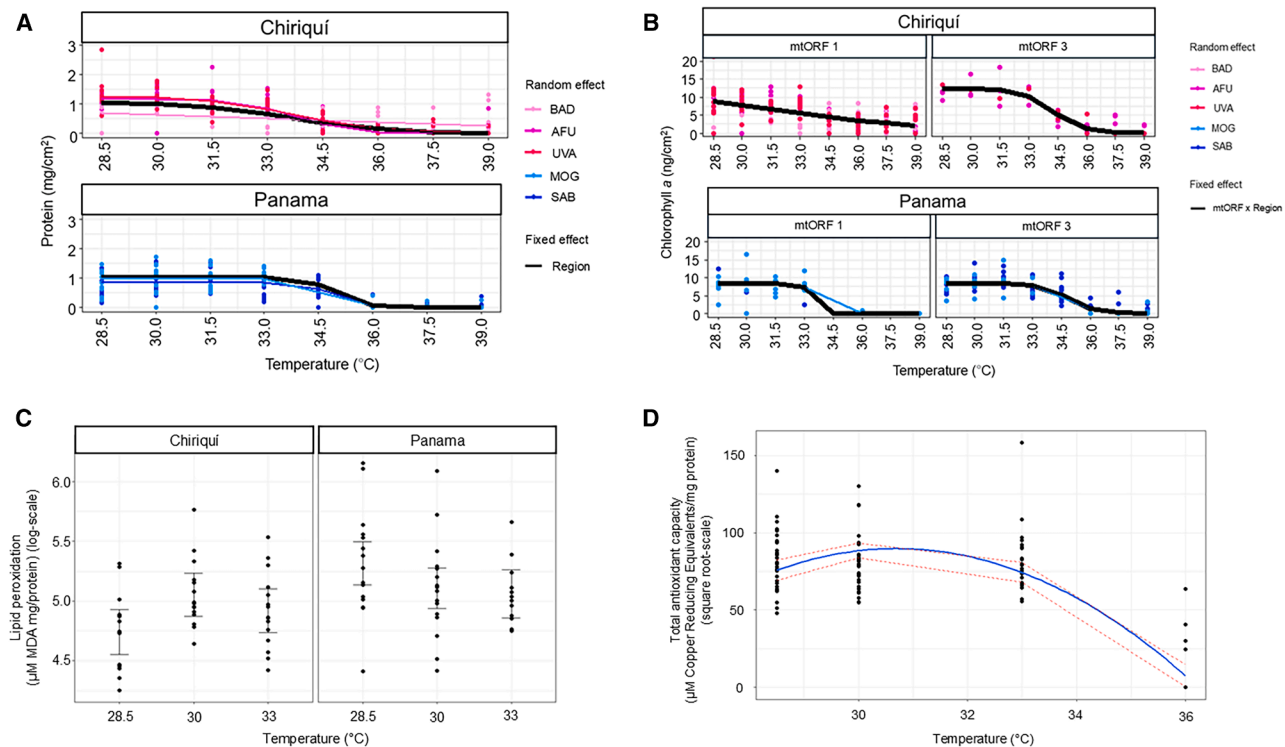


Figure 5. Physiological and oxidative metabolism dynamics for *Pocillopora* corals during the CBASS

Points represent predicted values.

(A) Predicted changes in host protein concentrations. The estimated gulf-level average responses (i.e., incorporating fixed effects) are shown as a black line, and the site-level responses (i.e., incorporating random effects of site) are shown as different colored lines.

(B) Predicted changes in chlorophyll *a* concentrations. The estimated average responses for the interaction of mtORF and region (i.e., incorporating fixed effects) are shown as a black line, and the site-level responses (i.e., incorporating random effects of site) are shown as different colored lines.

(C) Predicted changes in lipid peroxidation (LPO; expressed on a logarithmic scale). Three temperature treatments are examined: 28.5°C, 30°C, and 33°C, with 95% confidence intervals shown as a bar over each temperature treatment.

(D) Predicted changes in total antioxidant capacity (TAC; expressed on a square-root scale). Here four temperature treatments are examined: 28.5°C, 30°C, 33°C, and 36°C, with the 95% confidence interval shown as a red dotted line.

See [Data S2A–S2J](#) for model coefficients, results, and comparisons.

the CBASS experiment, thus further substantiating our prediction that upwelling is likely the factor most strongly driving bleaching trajectories across gulfs. By presenting how specific coral lineages interact differently with members of their microbiome, we deepen our understanding of the factors that influence thermotolerance, particularly within the context of reefs experiencing upwelling (cf. Randall et al.,⁷⁷ Rodriguez-Ruano et al.,⁷⁸ and Mayfield et al.⁷⁹).

Upwelling is resulting in divergent selection on genes implicated in thermotolerance

Based on *Fst* distributions between the Gulf of Panama and the Gulf of Chiriquí, only two outlier loci with protein-coding impacts were identified as being under putative divergent selection between gulfs. These two loci are located in genes that have been previously suggested to impact coral thermotolerance. The first variant is a predicted Rab-20-like protein, with this family of proteins playing various roles in signal trafficking pathways, including differentiating healthy and dysfunctional cells.^{85,86} This is expected to be important during bleaching-induced dysbiosis because it is hypothesized that these proteins play a central role

in the host's immune system by removing damaged symbionts.^{87–89} The second variant is a predicted hemicentin-2-like protein, a known extracellular matrix protein with important roles in tissue development. It has been proposed that this protein may be assisting corals in the Red Sea in persisting under high summer temperatures.^{90,91} These two loci show strong differentiation between gulfs despite high gene flow, suggesting that the distinct thermal history and upwelling regime of each gulf could be shaping heritable differences in coral thermotolerance in the TEP. Prior to our experiment, corals in the Gulf of Chiriquí experienced substantial bleaching as a result of the 2015–2016 El Niño Southern Oscillation (ENSO) event, while colonies in the Gulf of Panama did not, as upwelling coincided with periods of high-water temperatures. Outside the thermal refugia that upwelling may provide, higher temperatures in the Gulf of Chiriquí seem to be hampering coral cover and subsequent recovery.⁷⁷

Divergent microbiome responses to thermal stress suggest contrasting roles in coral thermotolerance

During the CBASS, *Cladocopium* spp. and *Durusdinium* spp. were the only two algal genera identified, in line with previous work

within this region (see Glynn et al.²⁵ and Palacio-Castro et al.²⁶). There is a well-documented shift to *Durusdinium*-dominated communities under heat stress, due presumably to these symbionts best assisting the host during bleaching^{26,50,92,93} (but see Turnham et al.⁹⁴). For studies in Panama's TEP, these insights have been gained from studying seasonal-to-interannual variation in *Pocillopora* colonies in the Gulf of Chiriquí. We have built upon this prior work by showing that during the CBASS, mtORF 3 colonies in the Gulf of Chiriquí had the greatest increases in *Durusdinium* spp., in line with the predictions of Palacio-Castro et al.²⁶ However, mtORF 3 corals in the Gulf of Panama had a more static *Cladocopium* spp.-dominated community throughout the assay, reflecting a less labile algal microbiome that may be driven by strong mtORF lineage specificity. Conversely, across both gulfs, mtORF 1 colonies from the onset of the CBASS were dominated by *Durusdinium* spp., and under thermal stress instead became *Cladocopium* spp. dominated, contrary to expectation (see Palacio-Castro et al.²⁶). Our data represent the most recent characterization of Panama's TEP algal communities. Thus, it is plausible that, given increasing seawater temperatures, previous predictions regarding *Durusdinium*-dominated microbiomes have already materialized. When considering chlorophyll *a* dynamics, mtORF 1 colonies in the Gulf of Panama, which showed the greatest relative increases in *Cladocopium* spp. by 36°C, had lower thermal thresholds than mtORF 3 colonies in the same gulf but higher thresholds than mtORF 1 colonies in the Gulf of Chiriquí. Therefore, it is plausible that the switch to *Cladocopium* spp. for mtORF 1 colonies at 36°C may occur if *Durusdinium* spp. is unable to satisfy the host's energy requirements, which is a trade-off previously reported.^{95,96} Thus, the greater relative proportions of *Cladocopium* spp. in mtORF 1 colonies at the highest temperatures may be due to selective loss of *Durusdinium* spp., and with no other compatible symbionts within the system, the coral could be prioritizing energy acquisition rather than thermotolerance. Investigation of this hypothesis via direct manipulation of the coral algal microbiome would be worthwhile. Our findings support previous work showing how the nuanced interaction between temperature and mtORF lineage potentially modulates Symbiodiniaceae dynamics under thermal stress and underscore the need to holistically assess host-microbiome interaction effects.^{26,50,92,93,97,98}

It is important to consider that, given the rapid nature of the CBASS, it is possible that slower-acting acclimatory and plastic effects were not captured, resulting in our observed mtORF-Symbiodiniaceae dynamics. For example, the rapid increases in temperature could have precluded photoacclimation of the resident algal symbionts, which has been a widely reported mechanism in longer-term experimental studies of coral thermotolerance.^{99–101} If so, the observed Symbiodiniaceae shifts may have diminished if there had been additional time for photoacclimation to occur, allowing the resident algal symbionts to support the host's energy requirements. It will be important for future research to test host-algal responses across additional timescales to ascertain the relative contributions of algal community shifts versus photoacclimatory dynamics during heat stress events.^{102–104}

Although we did not observe increases in community variance for the coral algal microbiome, there were temperature-driven community variance shifts for the prokaryotic community during the CBASS. The AKP proposes that increases in community variance for animal microbiomes under stress reflect a disease-like

state, because greater variance indicates the inability of the host and/or microbiome to regulate their community composition.⁸¹ Earlier AKP studies for cnidarians consider timescales on the order of months.^{83,84,105,106} Our findings support previous CBASS work by showing that drastic temperature-driven community dissimilarity shifts can occur on shorter time scales and do not appear to be impacted by genetic lineage or region (see Woolstra et al.⁵⁷). This is in contrast with previous studies on *Pocillopora* spp. in the Great Barrier Reef that have documented a relatively stable prokaryotic microbiome during bleaching stress.^{107–110} Yet these prior studies, which considered bleaching stress on the order of weeks to months, appear to represent less severe thermal stress than our CBASS experiments—e.g., with a mean monthly maximum (MMM) temperature of approximately 28.2°C in the Great Barrier Reef,¹¹¹ heat stress was ~4.3°C + MMM in Epstein et al.¹⁰⁹ and ~5.3°C + MMM in Bergman et al.¹⁰⁷ By contrast, with MMM across our sites in Panama's TEP being ~28.5°C, the prokaryotic shifts indicative of AKP in our experiment were not observed until the temperature anomaly reached ~7.5°C + MMM. This temperature is well above our estimated thermal physiological thresholds, suggesting that, at least for this genus, more severe stress may be required to trigger prokaryotic dysbiosis than to trigger physiological breakdown, perhaps in part due to the relatively stable nature of the *Pocillopora* microbiome (see Pogoreutz et al.¹¹⁰).

The strong contrast that we observed between *Pocillopora* coral's algal and prokaryotic communities during the CBASS may reflect the larger role of these communities for holobiont functioning. Although bleaching is by definition triggered by algal-host dysbiosis, we see shifts in algal communities over the course of our assay without corresponding increases in algal community variance. Therefore, the observed high stochasticity of prokaryotic communities may indicate that these microbiome members are less likely than their algal counterparts to complement the host's existing response pathways to thermal stress.^{112–114} An alternate explanation is plausible: given we visually observed a high degree of tissue loss past 36°C, the prokaryotic shifts during our assay may be capturing a gradual shift toward a different component of the coral supplying the majority of the sampled microbiome (e.g., from tissue to skeleton). Corals' tissue, mucus, and skeleton microbes differ from one another in terms of their prokaryotic richness and composition, with the skeleton endolith communities being especially diverse.^{115–118} Because we confined our sampling to temperatures below those at which visually apparent tissue sloughing occurred, we do not think that these microbiome dynamics are driven principally by differential losses of particular tissue components of the coral microbiome. However, we recognize that some sloughing still may have occurred at 36°C. If this occurred differentially among colonies, then it could have contributed to the higher variance (e.g., some colonies more dominated by skeletal microbiomes, with others retaining more of other tissue compartments).

Region, mtORF lineage, and temperature shape host physiology and oxidative metabolism dynamics during thermal stress

The suite of physiological and oxidative metabolism metrics measured during the CBASS complements our microbial data and further substantiates how region and mtORF

lineage are potentially shaping TEP *Pocillopora* thermotolerance. Although these parameters have been explored during longer-term abiotic stress experiments with coral populations, including during experimental simulations of upwelling,^{35,37,38,119} few studies have incorporated them into an acute thermal stress assay (but see Voolstra et al.⁶⁴). Although less commonly reported than traditional bleaching descriptors (i.e., symbiont density, chlorophyll *a*, and host protein concentrations), oxidative stress metrics can provide an added perspective to understanding the tolerable levels of bleaching stress.^{36,120,121} Our models of host-derived metrics suggest that *Pocillopora* corals from the Gulf of Panama experience a more demanding environment to maintain their redox balance (shown by the higher baseline levels of LPO), in turn resulting in an overall improved ability to counteract oxidative stress damage (LPO) and physiologically resist thermal stress (protein). It is possible that tissue sloughing contributes to some of the physiological and biochemical responses measured during our assay, but it is not likely the strongest driver of our observed trends. This is because the physiological model's predicted declines as a function of temperature (see [Figures 5A and 5B](#)), and thus our estimated model parameters of interest, are predominantly driven by the dynamics at temperatures that preceded significant tissue sloughing in the assay (below 36°C). Interestingly, the similar functional responses of protein and chlorophyll *a* concentrations to temperature in our assay contrast with some of the results obtained by Voolstra et al.,⁶⁴ who found that tissue protein content varied among sites but not with temperature treatment, whereas chlorophyll *a* resolved temperature-specific differences. On this basis they proposed that tissue protein content may not be an ideal biomarker for acute thermal stress such as that imposed by the CBASS' experimental design. Given the close correspondence between protein and chlorophyll *a* concentration responses in our assay, we believe that the utility of protein content as a metric of short-term thermal stress warrants further investigation. While differences due to region and study species may be factors in the differences between our results and those of Voolstra et al.,⁶⁴ it is also possible that our log-logistic modeling approach and the granularity of our temperature treatments (eight temperatures versus four in Voolstra et al.⁶⁴) increased our power to detect tissue protein content responses to temperature.

Our chlorophyll *a* model was the only model for which we found support for mtORF-driven differences in physiological condition. mtORF 1 colonies experienced sharper declines in this parameter, with this pattern being more pronounced for colonies from the Gulf of Panama. Our work provides new insights into coral lineage-environment interactions by showing how seasonal upwelling can significantly shape coral holobiont configurations and their physiological and biochemical responses to thermal stress.^{122–125} Lastly, contrary to our expectations, the best model for TAC was solely driven by temperature, in contrast to the region- and mtORF-specific patterns observed for other metrics, although our power to identify other differences may be reduced as only four temperatures, rather than eight (cf. protein, chlorophyll *a*), were analyzed.

Panama's TEP as a natural laboratory for coral holobiont research

Panama's TEP has historically served as a natural laboratory for studies on coral thermotolerance, with some of the first evidence on the role of microbial dynamics in bleaching emerging from studying these reefs.^{25,126} Previous research in the TEP has been mostly observational in nature^{127–132} (but see D'Croz and Maté⁶¹), which we have built upon by subjecting corals from both gulfs to an acute thermal stress assay and, in the process, exploring a diversity of host and microbiome mechanisms underlying thermotolerance. We found support for mtORF-specific responses to thermal stress during the CBASS, with mtORF 3 colonies across both gulfs showing the highest resistance to acute thermal stress, in contrast with previously reported long-term dynamics.²⁶ Importantly, by having physiological data for the host, we were able to ascertain potential fitness costs associated with increases in the relative abundance of *Cladocopium* spp. for mtORF 1 colonies. Our physiological and oxidative metabolism measurements support previous findings that corals in the Gulf of Panama are best able to cope with increasing thermal stress.⁷⁷ In leveraging the unique upwelling regime in Panama's TEP, our work shows how host and microbiome responses complement each other during bleaching and how these configurations are shaped by the environment, thereby providing an integrated view of the mechanisms that drive differences in coral thermotolerance.

RESOURCE AVAILABILITY

Lead contact

Further information and requests for resources should be directed to and will be fulfilled by the lead contact, Victoria Marie Glynn (victoria.glynn@mail.mcgill.ca).

Materials availability

This study did not generate unique materials.

Data and code availability

- Raw data from whole genome, microbiome marker gene, and mtORF sequencing have been deposited in the National Center for Biotechnology Information (NCBI) (<https://www.ncbi.nlm.nih.gov/>). Accession numbers are listed in the [key resources table](#).
- All original code and R scripts and our physiology and oxidative metabolism data are available at <https://doi.org/10.5281/zenodo.15532242>.
- Any additional information required to reanalyze the data reported in this paper is available from the [lead contact](#) upon request.

ACKNOWLEDGMENTS

Support was provided by a Mark and Rachel Rohr Foundation grant for the Rohr Reef Resilience Project (D.I.K., M.L., and S.R.C.), a Fulbright US Scholars Program grant (V.M.G.), a Vanier Canada Graduate Scholarship (V.M.G.), an NSERC Collaborative Research and Training Experience (CREATE) in Biodiversity, Ecosystem Services and Sustainability (V.M.G.), a Smithsonian Tropical Research Institute Short-Term Fellowship (V.M.G.), and an NSERC Discovery Grant and Canada Research Chair (R.D.H.B.). We thank Anabell Cornejo for her support during the field collections and Daniel Barshis for invaluable advice regarding the experimental system setup. We thank Pascale Marquis, Emmanuel Gonzales, Gary Leveque, Michael Connelly, and Ninoska Adam for help with the data analyses. We thank Antoine Paccard, Janick St-Cyr, Marta Vargas, and Eyda Gomez for their support in preparing and sequencing the associated libraries. We thank Rodney Arosemena, Analía Guerrero, and Daviana Berkowitz-Sklar for their assistance during the experiments and lab analyses.

AUTHOR CONTRIBUTIONS

V.M.G., L.F.d.B.M., D.I.K., M.L., S.R.C., and R.D.H.B. designed the study. V.M.G., L.F.d.B.M., H.Q., M.Y., D.I.K., M.L., and S.R.C. performed the acute thermal stress assay and data collection. V.M.G. and L.F.d.B.M. led the laboratory analyses, with support from E.R.T., V.A., H.Q., E.C.R.G., and M.L. V.M.G. led the statistical analyses, with support from M.G. and with guidance from S.R.C. and R.D.H.B. R.D.H.B. supervised V.M.G.'s work on the project, with co-supervision from D.I.K. and S.R.C. at different stages. V.M.G. wrote the manuscript with substantive contributions from L.F.d.B.M., M.L., S.R.C., and R.D.H.B.

DECLARATION OF INTERESTS

The authors declare no competing interests.

STAR★METHODS

Detailed methods are provided in the online version of this paper and include the following:

- KEY RESOURCES TABLE
- EXPERIMENTAL MODEL AND STUDY PARTICIPANT DETAILS
 - Field collections
- METHOD DETAILS
 - Host population genetics
 - SNP-by-genotyping
 - Acute thermal stress assay
 - Microbiome characterization
 - Physiological measurements
 - Oxidative metabolism measurements
- QUANTIFICATION AND STATISTICAL ANALYSES
 - Microbiome characterization
 - Physiological measurements
 - Oxidative metabolism

SUPPLEMENTAL INFORMATION

Supplemental information can be found online at <https://doi.org/10.1016/j.cub.2025.05.035>.

Received: September 10, 2024

Revised: February 4, 2025

Accepted: May 14, 2025

Published: June 5, 2025

REFERENCES

1. Oostra, V., Saastamoinen, M., Zwaan, B.J., and Wheat, C.W. (2018). Strong phenotypic plasticity limits potential for evolutionary responses to climate change. *Nat. Commun.* *9*, 1005. <https://doi.org/10.1038/s41467-018-03384-9>.
2. Richter, S., Kipfer, T., Wohlgenuth, T., Calderón Guerrero, C., Ghazoul, J., and Moser, B. (2012). Phenotypic plasticity facilitates resistance to climate change in a highly variable environment. *Oecologia* *169*, 269–279. <https://doi.org/10.1007/s00442-011-2191-x>.
3. Bitter, M.C., Kapsenberg, L., Gattuso, J.P., and Pfister, C.A. (2019). Standing genetic variation fuels rapid adaptation to ocean acidification. *Nat. Commun.* *10*, 5821. <https://doi.org/10.1038/s41467-019-13767-1>.
4. Des Roches, S., Bell, M.A., and Palkovacs, E.P. (2020). Climate-driven habitat change causes evolution in Threespine Stickleback. *Glob. Change Biol.* *26*, 597–606. <https://doi.org/10.1111/gcb.14892>.
5. Richardson, B.A., Chaney, L., Shaw, N.L., and Still, S.M. (2017). Will phenotypic plasticity affecting flowering phenology keep pace with climate change? *Glob. Change Biol.* *23*, 2499–2508. <https://doi.org/10.1111/gcb.13532>.
6. Bastille-Rousseau, G., Schaefer, J.A., Peers, M.J.L., Ellington, E.H., Mumma, M.A., Rayl, N.D., Mahoney, S.P., and Murray, D.L. (2018). Climate change can alter predator–prey dynamics and population viability of prey. *Oecologia* *186*, 141–150. <https://doi.org/10.1007/s00442-017-4017-y>.
7. Peers, M.J.L., Majchrzak, Y.N., Menzies, A.K., Studd, E.K., Bastille-Rousseau, G., Boonstra, R., Humphries, M., Jung, T.S., Kenney, A.J., Krebs, C.J., et al. (2020). Climate change increases predation risk for a keystone species of the boreal forest. *Nat. Clim. Change* *10*, 1149–1153. <https://doi.org/10.1038/s41558-020-00908-4>.
8. Alexander, J.M., Diez, J.M., and Levine, J.M. (2015). Novel competitors shape species' responses to climate change. *Nature* *525*, 515–518. <https://doi.org/10.1038/nature14952>.
9. Ettinger, A., and HilleRisLambers, J. (2017). Competition and facilitation may lead to asymmetric range shift dynamics with climate change. *Glob. Change Biol.* *23*, 3921–3933. <https://doi.org/10.1111/gcb.13649>.
10. Margulis, L., and Fester, R. (1991). *Symbiosis as a Source of Evolutionary Innovation: Speciation and Morphogenesis* (MIT Press).
11. Rosenberg, E., and Zilber-Rosenberg, I. (2018). The hologenome concept of evolution after 10 years. *Microbiome* *6*, 78. <https://doi.org/10.1186/s40168-018-0457-9>.
12. Roughgarden, J. (2023). Holobiont Evolution: Population Theory for the Hologenome. *Am. Nat.* *201*, 763–778. <https://doi.org/10.1086/723782>.
13. McFall-Ngai, M., Hadfield, M.G., Bosch, T.C.G., Carey, H.V., Domazet-Lošo, T., Douglas, A.E., Dubilier, N., Eberl, G., Fukami, T., Gilbert, S.F., et al. (2013). Animals in a bacterial world, a new imperative for the life sciences. *Proc. Natl. Acad. Sci. USA* *110*, 3229–3236. <https://doi.org/10.1073/pnas.1218525110>.
14. Voolstra, C.R., Raina, J.-B., Dörr, M., Cárdenas, A., Pogoreutz, C., Silveira, C.B., Mohamed, A.R., Bourne, D.G., Luo, H., Amin, S.A., et al. (2024). The coral microbiome in sickness, in health and in a changing world. *Nat. Rev. Microbiol.* *22*, 460–475. <https://doi.org/10.1038/s41579-024-01015-3>.
15. Trivedi, P., Leach, J.E., Tringe, S.G., Sa, T., and Singh, B.K. (2020). Plant–microbiome interactions: From community assembly to plant health. *Nat. Rev. Microbiol.* *18*, 607–621. <https://doi.org/10.1038/s41579-020-0412-1>.
16. Voolstra, C.R., Suggett, D.J., Peixoto, R.S., Parkinson, J.E., Quigley, K.M., Silveira, C.B., Sweet, M., Muller, E.M., Barshis, D.J., Bourne, D.G., et al. (2021). Extending the natural adaptive capacity of coral holobionts. *Nat. Rev. Earth Environ.* *2*, 747–762. <https://doi.org/10.1038/s43017-021-00214-3>.
17. Grottolli, A.G., Dalcin Martins, P.D., Wilkins, M.J., Johnston, M.D., Warner, M.E., Cai, W.-J., Melman, T.F., Hoadley, K.D., Pettay, D.T., Levas, S., et al. (2018). Coral physiology and microbiome dynamics under combined warming and ocean acidification. *PLoS One* *13*, e0191156. <https://doi.org/10.1371/journal.pone.0191156>.
18. Marchioro, G.M., Glasl, B., Engelen, A.H., Serrão, E.A., Bourne, D.G., Webster, N.S., and Frade, P.R. (2020). Microbiome dynamics in the tissue and mucus of acroporid corals differ in relation to host and environmental parameters. *PeerJ* *8*, e9644. <https://doi.org/10.7717/peerj.9644>.
19. Boilard, A., Dubé, C.E., Gruet, C., Mercière, A., Hernandez-Agreda, A., and Derome, N. (2020). Defining Coral Bleaching as a Microbial Dysbiosis within the Coral Holobiont. *Microorganisms* *8*, 11. <https://doi.org/10.3390/microorganisms8111682>.
20. van Oppen, M.J.H., and Blackall, L.L. (2019). Coral microbiome dynamics, functions and design in a changing world. *Nat. Rev. Microbiol.* *17*, 9. <https://doi.org/10.1038/s41579-019-0223-4>.
21. Bourne, D.G., Morrow, K.M., and Webster, N.S. (2016). Insights into the Coral Microbiome: Underpinning the Health and Resilience of Reef Ecosystems. *Annu. Rev. Microbiol.* *70*, 317–340. <https://doi.org/10.1146/annurev-micro-102215-095440>.
22. Ziegler, M., Seneca, F.O., Yum, L.K., Palumbi, S.R., and Voolstra, C.R. (2017). Bacterial community dynamics are linked to patterns of coral

- heat tolerance. *Nat. Commun.* 8, 14213. <https://doi.org/10.1038/ncomms14213>.
23. Davy, S.K., Allemand, D., and Weis, V.M. (2012). Cell Biology of Cnidarian-Dinoflagellate Symbiosis. *Microbiol. Mol. Biol. Rev.* 76, 229–261. <https://doi.org/10.1128/MMBR.05014-11>.
24. Weis, V.M. (2008). Cellular mechanisms of Cnidarian bleaching: Stress causes the collapse of symbiosis. *J. Exp. Biol.* 211, 3059–3066. <https://doi.org/10.1242/jeb.009597>.
25. Glynn, P., Mate, J., Baker, A., and Calderón, M. (2001). Coral bleaching and mortality in Panama and Ecuador during the 1997–1998 El Niño–Southern Oscillation event: Spatial/temporal patterns and comparisons with the 1982–1983 event. *Bull. Mar. Sci.* 69, 79–109.
26. Palacio-Castro, A.M., Smith, T.B., Brandtneris, V., Snyder, G.A., van Hooidonk, R., Maté, J.L., Manzello, D., Glynn, P.W., Fong, P., and Baker, A.C. (2023). Increased dominance of heat-tolerant symbionts creates resilient coral reefs in near-term ocean warming. *Proc. Natl. Acad. Sci. USA* 120, e2202388120. <https://doi.org/10.1073/pnas.2202388120>.
27. Meyer, J.L., Castellanos-Gell, J., Aeby, G.S., Häse, C.C., Ushijima, B., and Paul, V.J. (2019). Microbial Community Shifts Associated With the Ongoing Stony Coral Tissue Loss Disease Outbreak on the Florida Reef Tract. *Front. Microbiol.* 10, 2244. <https://doi.org/10.3389/fmicb.2019.02244>.
28. Vega Thurber, R.V., Willner-Hall, D., Rodriguez-Mueller, B., Desnues, C., Edwards, R.A., Angly, F., Dinsdale, E., Kelly, L., and Rohwer, F. (2009). Metagenomic analysis of stressed coral holobionts. *Environ. Microbiol.* 11, 2148–2163. <https://doi.org/10.1111/j.1462-2920.2009.01935.x>.
29. Zhang, Y., Ling, J., Yang, Q., Wen, C., Yan, Q., Sun, H., Van Nostrand, J. D., Shi, Z., Zhou, J., and Dong, J. (2015). The functional gene composition and metabolic potential of coral-associated microbial communities. *Sci. Rep.* 5, 1. <https://doi.org/10.1038/srep16191>.
30. Glasl, B., Herndl, G.J., and Frade, P.R. (2016). The microbiome of coral surface mucus has a key role in mediating holobiont health and survival upon disturbance. *ISME J.* 10, 9. <https://doi.org/10.1038/ismej.2016.9>.
31. Kline, D.I., and Vollmer, S.V. (2011). White Band Disease (type I) of Endangered Caribbean Acroporid Corals is Caused by Pathogenic Bacteria. *Sci. Rep.* 1, 7. <https://doi.org/10.1038/srep00007>.
32. Rosado, P.M., Leite, D.C.A., Duarte, G.A.S., Chaloub, R.M., Jospin, G., Nunes da Rocha, U., P Saraiva, J., Dini-Andreote, F., Eisen, J.A., Bourne, D.G., et al. (2019). Marine probiotics: Increasing coral resistance to bleaching through microbiome manipulation. *ISME J.* 13, 921–936. <https://doi.org/10.1038/s41396-018-0323-6>.
33. Santoro, E.P., Borges, R.M., Espinoza, J.L., Freire, M., Messias, C.S.M. A., Villela, H.D.M., Pereira, L.M., Vilela, C.L.S., Rosado, J.G., Cardoso, P. M., et al. (2021). Coral microbiome manipulation elicits metabolic and genetic restructuring to mitigate heat stress and evade mortality. *Sci. Adv.* 7, eabg3088. <https://doi.org/10.1126/sciadv.abg3088>.
34. Suggett, D.J., and Smith, D.J. (2020). Coral bleaching patterns are the outcome of complex biological and environmental networking. *Glob. Change Biol.* 26, 68–79. <https://doi.org/10.1111/gcb.14871>.
35. Fernandes de Barros Marangoni, L., Ferrier-Pagès, C., Rottier, C., Bianchini, A., and Grover, R. (2020). Unravelling the different causes of nitrate and ammonium effects on coral bleaching. *Sci. Rep.* 10, 11975. <https://doi.org/10.1038/s41598-020-68916-0>.
36. Lesser, M.P. (2024). Irradiance dependency of oxidative stress and coral bleaching. *Coral Reefs* 43, 1393–1403. <https://doi.org/10.1007/s00338-024-02545-1>.
37. Marangoni, L.F.B., Rottier, C., and Ferrier-Pagès, C. (2021). Symbiont regulation in *Stylophora pistillata* during cold stress: An acclimation mechanism against oxidative stress and severe bleaching. *J. Exp. Biol.* 224, jeb235275. <https://doi.org/10.1242/jeb.235275>.
38. Fernandes de Barros Marangoni, L., Dalmolin, C., Marques, J.A., Klein, R.D., Abrantes, D.P., Pereira, C.M., Calderon, E.N., Castro, C.B.E., and Bianchini, A. (2019). Oxidative stress biomarkers as potential tools in reef degradation monitoring: A study case in a South Atlantic reef under influence of the 2015–2016 El Niño/Southern Oscillation (ENSO). *Ecol. Indic.* 106, 105533. <https://doi.org/10.1016/j.ecolind.2019.105533>.
39. Liñán-Cabello, M.A., Flores-Ramírez, L.A., Zenteno-Savín, T., Olguin-Monroy, N.O., Sosa-Avalos, R., Patiño-Barragan, M., and Olivos-Ortiz, A. (2010). Seasonal changes of antioxidant and oxidative parameters in the coral *Pocillopora capitata* on the Pacific coast of Mexico. *Mar. Ecol.* 31, 407–417. <https://doi.org/10.1111/j.1439-0485.2009.00349.x>.
40. da Silva Fonseca, J., Mies, M., Paranhos, A., Taniguchi, S., Güth, A.Z., Bicego, M.C., Marques, J.A., Fernandes de Barros Marangoni, L., and Bianchini, A. (2021). Isolated and combined effects of thermal stress and copper exposure on the trophic behavior and oxidative status of the reef-building coral *Mussismilia harttii*. *Environ. Pollut.* 268, 115892. <https://doi.org/10.1016/j.envpol.2020.115892>.
41. Luz, D.C., Zebal, Y.D., Klein, R.D., Marques, J.A., Marangoni, L.F. de B., Pereira, C.M., Duarte, G.A.S., Pires, D. de O., Castro, C.B.E., Calderon, E.N., et al. (2018). Oxidative stress in the hydrocoral *Millepora alcicornis* exposed to CO₂-driven seawater acidification. *Coral Reefs* 37, 571–579. <https://doi.org/10.1007/s00338-018-1681-2>.
42. Rådecker, N., Escrig, S., Spangenberg, J.E., Voolstra, C.R., and Meibom, A. (2023). Coupled carbon and nitrogen cycling regulates the cnidarian–algal symbiosis. *Nat. Commun.* 14, 6948. <https://doi.org/10.1038/s41467-023-42579-7>.
43. Rådecker, N., Pogoreutz, C., Gegner, H.M., Cárdenas, A., Roth, F., Bougoure, J., Guagliardo, P., Wild, C., Pernice, M., Raina, J.-B., et al. (2021). Heat stress destabilizes symbiotic nutrient cycling in corals. *Proc. Natl. Acad. Sci. USA* 118, e2022653118. <https://doi.org/10.1073/pnas.2022653118>.
44. Schlottheuber, M., Voolstra, C.R., de Beer, D., Camp, E.F., Klatt, J.M., Ghilardi, M., Neumüller, K., Ousley, S., and Bejarano, S. (2024). High temporal resolution of hydrogen peroxide (H₂O₂) dynamics during heat stress does not support a causative role in coral bleaching. *Coral Reefs* 43, 119–133. <https://doi.org/10.1007/s00338-023-02448-7>.
45. Dungan, A.M., Maire, J., Perez-Gonzalez, A., Blackall, L.L., and van Oppen, M.J.H. (2022). Lack of evidence for the oxidative stress theory of bleaching in the sea anemone, *Exaiptasia diaphana*, under elevated temperature. *Coral Reefs* 41, 1161–1172. <https://doi.org/10.1007/s00338-022-02251-w>.
46. Barshis, D.J., Ladner, J.T., Oliver, T.A., Seneca, F.O., Traylor-Knowles, N., and Palumbi, S.R. (2013). Genomic basis for coral resilience to climate change. *Proc. Natl. Acad. Sci. USA* 110, 1387–1392. <https://doi.org/10.1073/pnas.1210224110>.
47. Brener-Raffalli, K., Vidal-Dupiol, J., Adjeroud, M., Rey, O., Romans, P., Bonhomme, F., Pralong, M., Haguenaue, A., Pillot, R., Feuillassier, L., et al. (2022). Gene expression plasticity and frontloading promote thermotolerance in *Pocillopora* corals. *Peer Community J.* 2, e13. <https://doi.org/10.24072/pcjournal.79>.
48. Collins, M., Clark, M.S., Spicer, J.I., and Truebano, M. (2021). Transcriptional frontloading contributes to cross-tolerance between stressors. *Evol. Appl.* 14, 577–587. <https://doi.org/10.1111/eva.13142>.
49. Strader, M.E., and Quigley, K.M. (2022). The role of gene expression and symbiosis in reef-building coral acquired heat tolerance. *Nat. Commun.* 13, 4513. <https://doi.org/10.1038/s41467-022-32217-z>.
50. Cunning, R., and Baker, A.C. (2020). Thermotolerant coral symbionts modulate heat stress-responsive genes in their hosts. *Mol. Ecol.* 29, 2940–2950. <https://doi.org/10.1111/mec.15526>.
51. Drury, C., Bean, N.K., Harris, C.I., Hancock, J.R., Huckeba, J., H, C.M., Roach, T.N.F., Quinn, R.A., and Gates, R.D. (2022). Intrapopulation adaptive variance supports thermal tolerance in a reef-building coral. *Commun. Biol.* 5, 486. <https://doi.org/10.1038/s42003-022-03428-3>.
52. Rose, N.H., Bay, R.A., Morikawa, M.K., and Palumbi, S.R. (2018). Polygenic evolution drives species divergence and climate adaptation in corals. *Evolution* 72, 82–94. <https://doi.org/10.1111/evo.13385>.
53. Bay, R.A., and Palumbi, S.R. (2014). Multilocus Adaptation Associated with Heat Resistance in Reef-Building Corals. *Curr. Biol.* 24, 2952–2956. <https://doi.org/10.1016/j.cub.2014.10.044>.

54. Yetsko, K., Ross, M., Bellantuono, A., Merselis, D., Rodriguez-Lanetty, M., and Gilg, M.R. (2020). Genetic differences in thermal tolerance among colonies of threatened coral *Acropora cervicornis*: Potential for adaptation to increasing temperature. *Mar. Ecol. Prog. Ser.* 646, 45–68. <https://doi.org/10.3354/meps13407>.
55. Dixon, G.B., Davies, S.W., Aglyamova, G.A., Meyer, E., Bay, L.K., and Matz, M.V. (2015). CORAL REEFS. Genomic determinants of coral heat tolerance across latitudes. *Science* 348, 1460–1462. <https://doi.org/10.1126/science.1261224>.
56. Smith, S.J., Mogensen, S., Barry, T.N., Paccard, A., Jamniczky, H.A., Barrett, R.D.H., and Rogers, S.M. (2022). Evolution of thermal physiology alters the projected range of threespine stickleback under climate change. *Mol. Ecol.* 31, 2312–2326. <https://doi.org/10.1111/mec.16396>.
57. Voolstra, C.R., Valenzuela, J.J., Turkarslan, S., Cárdenas, A., Hume, B.C., Perna, G., Buitrago-López, C., Rowe, K., Orellana, M.V., Baliga, N.S., et al. (2021). Contrasting heat stress response patterns of coral holobionts across the Red Sea suggest distinct mechanisms of thermal tolerance. *Mol. Ecol.* 30, 4466–4480. <https://doi.org/10.1111/mec.16064>.
58. Oliver, T.A., and Palumbi, S.R. (2011). Do fluctuating temperature environments elevate coral thermal tolerance? *Coral Reefs* 30, 429–440. <https://doi.org/10.1007/s00338-011-0721-y>.
59. Starko, S., Fifer, J.E., Claar, D.C., Davies, S.W., Cuning, R., Baker, A.C., and Baum, J.K. (2023). Marine heatwaves threaten cryptic coral diversity and erode associations among coevolving partners. *Sci. Adv.* 9, eadf0954. <https://doi.org/10.1126/sciadv.adf0954>.
60. Rodríguez-Casariago, J.A., Mercado-Molina, A.E., Garcia-Souto, D., Ortiz-Rivera, I.M., Lopes, C., Baums, I.B., Sabat, A.M., and Eirin-Lopez, J.M. (2020). Genome-Wide DNA Methylation Analysis Reveals a Conserved Epigenetic Signature to Seasonal Environmental Variation in the Staghorn Coral *Acropora cervicornis*. *Front. Mar. Sci.* 7, 560424. <https://doi.org/10.3389/fmars.2020.560424>.
61. D’Croz, L., and Maté, J.L. (2004). Experimental responses to elevated water temperature in genotypes of the reef coral *Pocillopora damicornis* from upwelling and non-upwelling environments in Panama. *Coral Reefs* 23, 473–483. <https://doi.org/10.1007/s00338-004-0397-7>.
62. Kenkel, C.D., Goodbody-Gringley, G., Caillaud, D., Davies, S.W., Bartels, E., and Matz, M.V. (2013). Evidence for a host role in thermotolerance divergence between populations of the mustard hill coral (*Porites astreoides*) from different reef environments. *Mol. Ecol.* 22, 4335–4348. <https://doi.org/10.1111/mec.12391>.
63. Gardner, S.G., Raina, J.-B., Nitschke, M.R., Nielsen, D.A., Stat, M., Motti, C.A., Ralph, P.J., and Petrou, K. (2017). A multi-trait systems approach reveals a response cascade to bleaching in corals. *BMC Biol.* 15, 117. <https://doi.org/10.1186/s12915-017-0459-2>.
64. Voolstra, C.R., Buitrago-López, C., Perna, G., Cárdenas, A., Hume, B.C., Rådecker, N., and Barshis, D.J. (2020). Standardized short-term acute heat stress assays resolve historical differences in coral thermotolerance across microhabitat reef sites. *Glob. Change Biol.* 26, 4328–4343. <https://doi.org/10.1111/gcb.15148>.
65. Evensen, N.R., Parker, K.E., Oliver, T.A., Palumbi, S.R., Logan, C.A., Ryan, J.S., Klepac, C.N., Perna, G., Warner, M.E., Voolstra, C.R., et al. (2023). The Coral Bleaching Automated Stress System (CBASS): A low-cost, portable system for standardized empirical assessments of coral thermal limits. *Limnol. Oceanogr.: Methods* 21, 421–434. <https://doi.org/10.1002/lom3.10555>.
66. Voolstra, C.R., Alderdice, R., Colin, L., Staab, S., Apprill, A., and Raina, J.-B. (2025). Standardized Methods to Assess the Impacts of Thermal Stress on Coral Reef Marine Life. *Ann. Rev. Mar. Sci.* 17, 193–226. <https://doi.org/10.1146/annurev-marine-032223-024511>.
67. Romero-Torres, M., Acosta, A., Palacio-Castro, A.M., Tremli, E.A., Zapata, F.A., Paz-García, D.A., and Porter, J.W. (2020). Coral reef resilience to thermal stress in the Eastern Tropical Pacific. *Glob. Change Biol.* 26, 3880–3890. <https://doi.org/10.1111/gcb.15126>.
68. Manzello, D.P., Kleypas, J.A., Budd, D.A., Eakin, C.M., Glynn, P.W., and Langdon, C. (2008). Poorly cemented coral reefs of the eastern tropical Pacific: Possible insights into reef development in a high-CO₂ world. *Proc. Natl. Acad. Sci. USA* 105, 10450–10455. <https://doi.org/10.1073/pnas.0712167105>.
69. Leray, M., Wilkins, L.G.E., Apprill, A., Bik, H.M., Clever, F., Connolly, S.R., De León, M.E.D., Duffy, J.E., Ezzat, L., Gignoux-Wolfsohn, S., et al. (2021). Natural experiments and long-term monitoring are critical to understand and predict marine host–microbe ecology and evolution. *PLoS Biol.* 19, e3001322. <https://doi.org/10.1371/journal.pbio.3001322>.
70. Glynn, P.W. (1993). Coral reef bleaching: Ecological perspectives. *Coral Reefs* 12, 1–17. <https://doi.org/10.1007/BF00303779>.
71. Glynn, P.W. (1983). Extensive ‘Bleaching’ and Death of Reef Corals on the Pacific Coast of Panamá. *Environ. Conserv.* 10, 149–154. <https://doi.org/10.1017/S0376892900012248>.
72. Crawford, G., Mepstead, M., and Díaz-Ferguson, E. (2024). Characterizing oceanographic conditions near Coiba Island and Pacific Panama using 20 years of satellite-based wind stress, SST and chlorophyll-*a* measurements. *Mar. Fish. Sci.* 37, 3. <https://doi.org/10.47193/mafis.37X2024010112>.
73. O’Dea, A., Hoyos, N., Rodríguez, F., Degracia, B., and De Gracia, C. (2012). History of upwelling in the Tropical Eastern Pacific and the paleogeography of the Isthmus of Panama. *Palaeogeogr. Palaeoclimatol. Palaeoecol.* 348–349, 59–66. <https://doi.org/10.1016/j.palaeo.2012.06.007>.
74. D’Croz, L., and O’Dea, A. (2007). Variability in upwelling along the Pacific shelf of Panama and implications for the distribution of nutrients and chlorophyll. *Estuarine Coastal Shelf Sci.* 73, 325–340. <https://doi.org/10.1016/j.ecss.2007.01.013>.
75. Chollett, I., Mumby, P., and Cortés, J. (2010). Upwelling areas do not guarantee refuge for coral reefs in a warming ocean. *Mar. Ecol. Prog. Ser.* 416, 47–56. <https://doi.org/10.3354/meps08775>.
76. Smith, T.B., Maté, J.L., and Gyory, J. (2017). Thermal Refuges and Refugia for Stony Corals in the Eastern Tropical Pacific. In *Coral Reefs of the Eastern Tropical Pacific*, 8, P.W. Glynn, D.P. Manzello, and I.C. Enochs, eds. (Springer), pp. 501–515. https://doi.org/10.1007/978-94-017-7499-4_17.
77. Randall, C.J., Toth, L.T., Leichter, J.J., Maté, J.L., and Aronson, R.B. (2020). Upwelling buffers climate change impacts on coral reefs of the eastern tropical Pacific. *Ecology* 101, e02918. <https://doi.org/10.1002/ecy.2918>.
78. Rodriguez-Ruano, V., Toth, L.T., Enochs, I.C., Randall, C.J., and Aronson, R.B. (2023). Upwelling, climate change, and the shifting geography of coral reef development. *Sci. Rep.* 13, 1770. <https://doi.org/10.1038/s41598-023-28489-0>.
79. Mayfield, A.B., Fan, T.-Y., and Chen, C.-S. (2013). Physiological acclimation to elevated temperature in a reef-building coral from an upwelling environment. *Coral Reefs* 32, 909–921. <https://doi.org/10.1007/s00338-013-1067-4>.
80. Zhu, W., Liu, X., Zhu, M., Xia, J., Chen, R., and Li, X. (2023). Coastal Upwelling Under Anthropogenic Influence Drives the Community Change, Assembly Process, and Co-Occurrence Pattern of Coral Associated Microorganisms. *JGR Oceans* 128, e2022JC019307. <https://doi.org/10.1029/2022JC019307>.
81. Zaneveld, J.R., McMinds, R., and Vega Thurber, R. (2017). Stress and stability: Applying the Anna Karenina principle to animal microbiomes. *Nat. Microbiol.* 2, 9. <https://doi.org/10.1038/nmicrobiol.2017.121>.
82. Alexander, D.H., and Lange, K. (2011). Enhancements to the ADMIXTURE algorithm for individual ancestry estimation. *BMC Bioinformatics* 12, 246. <https://doi.org/10.1186/1471-2105-12-246>.
83. Wang, L., Shantz, A.A., Payet, J.P., Sharpton, T.J., Foster, A., Burkepille, D.E., and Vega Thurber, R. (2018). Corals and Their Microbiomes Are Differentially Affected by Exposure to Elevated Nutrients and a Natural Thermal Anomaly. *Front. Mar. Sci.* 5. <https://doi.org/10.3389/fmars.2018.00101>.

84. Bourne, D., Iida, Y., Uthicke, S., and Smith-Keune, C. (2008). Changes in coral-associated microbial communities during a bleaching event. *ISME J.* 2, 350–363. <https://doi.org/10.1038/ismej.2007.112>.
85. Gutierrez, M.G. (2013). Functional role(s) of phagosomal Rab GTPases. *Small GTPases* 4, 148–158. <https://doi.org/10.4161/srgtp.25604>.
86. Bhui, T., and Roy, J.K. (2014). Rab proteins: The key regulators of intracellular vesicle transport. *Exp. Cell Res.* 328, 1–19. <https://doi.org/10.1016/j.yexcr.2014.07.027>.
87. Chen, M.-C., Hong, M.-C., Huang, Y.-S., Liu, M.-C., Cheng, Y.-M., and Fang, L.-S. (2005). ApRab11, a cnidarian homologue of the recycling regulatory protein Rab11, is involved in the establishment and maintenance of the *Aiptasia-Symbiodinium* endosymbiosis. *Biochem. Biophys. Res. Commun.* 338, 1607–1616. <https://doi.org/10.1016/j.bbrc.2005.10.133>.
88. Yuyama, I., Ishikawa, M., Nozawa, M., Yoshida, M.A., and Ikeo, K. (2018). Transcriptomic changes with increasing algal symbiont reveal the detailed process underlying establishment of coral-algal symbiosis. *Sci. Rep.* 8, 1. <https://doi.org/10.1038/s41598-018-34575-5>.
89. Traylor-Knowles, N., Connelly, M.T., Young, B.D., Eaton, K., Muller, E.M., Paul, V.J., Ushijima, B., DeMerlis, A., Drown, M.K., Goncalves, A., et al. (2021). Gene Expression Response to Stony Coral Tissue Loss Disease Transmission in *M. cavernosa* and *O. faveolata* From Florida. *Front. Mar. Sci.* 8, 681563. <https://doi.org/10.3389/fmars.2021.681563>.
90. Feitosa, N.M., Zhang, J., Carney, T.J., Metzger, M., Korzh, V., Bloch, W., and Hammerschmidt, M. (2012). Hemicentin 2 and Fibulin 1 are required for epidermal–dermal junction formation and fin mesenchymal cell migration during zebrafish development. *Dev. Biol.* 369, 235–248. <https://doi.org/10.1016/j.ydbio.2012.06.023>.
91. Gianakas, C.A., Keeley, D.P., Ramos-Lewis, W., Park, K., Jayadev, R., Kenny, I.W., Chi, Q., and Sherwood, D.R. (2023). Hemicentin-mediated type IV collagen assembly strengthens juxtaposed basement membrane linkage. *J. Cell Biol.* 222, e202112096. <https://doi.org/10.1083/jcb.202112096>.
92. Kemp, D.W., Hoadley, K.D., Lewis, A.M., Wham, D.C., Smith, R.T., Warner, M.E., and LaJeunesse, T.C. (2023). Thermotolerant coral–algal mutualisms maintain high rates of nutrient transfer while exposed to heat stress. *Proc. Biol. Sci.* 290, 20231403. <https://doi.org/10.1098/rspb.2023.1403>.
93. Claar, D.C., Starko, S., Tietjen, K.L., Epstein, H.E., Cuning, R., Cobb, K. M., Baker, A.C., Gates, R.D., and Baum, J.K. (2020). Dynamic symbioses reveal pathways to coral survival through prolonged heatwaves. *Nat. Commun.* 11, 6097. <https://doi.org/10.1038/s41467-020-19169-y>.
94. Turnham, K.E., Aschaffenburg, M.D., Pettay, D.T., Paz-García, D.A., Reyes-Bonilla, H., Pinzón, J., Timmins, E., Smith, R.T., McGinley, M.P., Warner, M.E., et al. (2023). High physiological function for corals with thermally tolerant, host-adapted symbionts. *Proc. Biol. Sci.* 290, 20231021. <https://doi.org/10.1098/rspb.2023.1021>.
95. Cantin, N.E., van Oppen, M.J.H., Willis, B.L., Mieog, J.C., and Negri, A.P. (2009). Juvenile corals can acquire more carbon from high-performance algal symbionts. *Coral Reefs* 28, 405–414. <https://doi.org/10.1007/s00338-009-0478-8>.
96. Allen-Waller, L., and Barott, K.L. (2023). Symbiotic dinoflagellates divert energy away from mutualism during coral bleaching recovery. *Symbiosis* 89, 173–186. <https://doi.org/10.1007/s13199-023-00901-3>.
97. LaJeunesse, T.C., Thornhill, D.J., Cox, E.F., Stanton, F.G., Fitt, W.K., and Schmidt, G.W. (2004). High diversity and host specificity observed among symbiotic dinoflagellates in reef coral communities from Hawaii. *Coral Reefs* 23, 596–603. <https://doi.org/10.1007/s00338-004-0428-4>.
98. Baker, A.C. (2003). Flexibility and Specificity in Coral-Algal Symbiosis: Diversity, Ecology, and Biogeography of *Symbiodinium*. *Annu. Rev. Ecol. Evol. Syst.* 34, 661–689. <https://doi.org/10.1146/annurev.ecolsys.34.011802.132417>.
99. Takahashi, S., Yoshioka-Nishimura, M., Nanba, D., and Badger, M.R. (2013). Thermal Acclimation of the Symbiotic Alga *Symbiodinium* spp. Alleviates Photobleaching under Heat Stress. *Plant Physiol.* 161, 477–485. <https://doi.org/10.1104/pp.112.207480>.
100. Quigley, K.M., Alvarez-Roa, C., Raina, J.-B., Pernice, M., and Van Oppen, M.J.H. (2023). Heat-evolved microalgal symbionts increase thermal bleaching tolerance of coral juveniles without a trade-off against growth. *Coral Reefs* 42, 1227–1232. <https://doi.org/10.1007/s00338-023-02426-z>.
101. Buerger, P., Alvarez-Roa, C., Coppin, C.W., Pearce, S.L., Chakravarti, L. J., Oakeshott, J.G., Edwards, O.R., and van Oppen, M.J.H. (2020). Heat-evolved microalgal symbionts increase coral bleaching tolerance. *Sci. Adv.* 6, eaba2498. <https://doi.org/10.1126/sciadv.aba2498>.
102. Crespi, B.J. (2000). The evolution of maladaptation. *Heredity* 84, 623–629. <https://doi.org/10.1046/j.1365-2540.2000.00746.x>.
103. Lohr, K.E., Camp, E.F., Kuzhiumparambil, U., Lutz, A., Leggat, W., Patterson, J.T., and Suggett, D.J. (2019). Resolving coral photoacclimation dynamics through coupled photophysiological and metabolomic profiling. *J. Exp. Biol.* 222, jeb195982. <https://doi.org/10.1242/jeb.195982>.
104. Klepac, C.N., Petrik, C.G., Karabelas, E., Owens, J., Hall, E.R., and Muller, E.M. (2024). Assessing acute thermal assays as a rapid screening tool for coral restoration. *Sci. Rep.* 14, 1898. <https://doi.org/10.1038/s41598-024-51944-5>.
105. Ahmed, H.I., Herrera, M., Liew, Y.J., and Aranda, M. (2019). Long-Term Temperature Stress in the Coral Model *Aiptasia* Supports the “Anna Karenina Principle” for Bacterial Microbiomes. *Front. Microbiol.* 10, 975. <https://doi.org/10.3389/fmicb.2019.00975>.
106. Greene, A., Moriarty, T., Leggat, W., Ainsworth, T.D., Donahue, M.J., and Raymundo, L. (2023). Spatial extent of dysbiosis in the branching coral *Pocillopora damicornis* during an acute disease outbreak. *Sci. Rep.* 13, 16522. <https://doi.org/10.1038/s41598-023-43490-3>.
107. Bergman, J.L., Leggat, W., and Ainsworth, T.D. (2021). The Meta-Organism Response of the Environmental Generalist *Pocillopora damicornis* Exposed to Differential Accumulation of Heat Stress. *Front. Mar. Sci.* 8, 1819. <https://doi.org/10.3389/fmars.2021.664063>.
108. Bergman, J.L., Ricci, F., Leggat, W., and Ainsworth, T.D. (2023). Characteristics of The Bleached Microbiome of The Generalist Coral *Pocillopora damicornis* from Two Distinct Reef Habitats. *Integr. Org. Biol.* 5, obad012. <https://doi.org/10.1093/iob/obad012>.
109. Epstein, H.E., Torda, G., and van Oppen, M.J.H. (2019). Relative stability of the *Pocillopora acuta* microbiome throughout a thermal stress event. *Coral Reefs* 38, 373–386. <https://doi.org/10.1007/s00338-019-01783-y>.
110. Pogoreutz, C., Rådecker, N., Cárdenas, A., Gärdes, A., Wild, C., and Voolstra, C.R. (2018). Dominance of *Endozoicomonas* bacteria throughout coral bleaching and mortality suggests structural inflexibility of the *Pocillopora verrucosa* microbiome. *Ecol. Evol.* 8, 2240–2252. <https://doi.org/10.1002/ece3.3830>.
111. NOAA Coral Reef Watch (2024). NOAA Coral Reef Watch Version 3.1 Daily 5km Satellite Regional Virtual Station Time Series Data for Northern Coral Sea Islands, 2023-2024. updated daily (NOAA Coral Reef Watch). <https://coralreefwatch.noaa.gov/product/vs/data.php>.
112. Howe-Kerr, L.I., Bachelot, B., Wright, R.M., Kenkel, C.D., Bay, L.K., and Correa, A.M.S. (2020). Symbiont community diversity is more variable in corals that respond poorly to stress. *Glob. Change Biol.* 26, 2220–2234. <https://doi.org/10.1111/gcb.14999>.
113. Díaz-Almeyda, E.M., Ryba, T., Ohdera, A.H., Collins, S.M., Shafer, N., Link, C., Prado-Zapata, M., Ruhnke, C., Moore, M., González Angel, A. M., et al. (2022). Thermal Stress Has Minimal Effects on Bacterial Communities of Thermotolerant *Symbiodinium* Cultures. *Front. Ecol. Evol.* 10, 764086. <https://doi.org/10.3389/fevo.2022.764086>.
114. Voolstra, C.R., and Ziegler, M. (2020). Adapting with Microbial Help: Microbiome Flexibility Facilitates Rapid Responses to Environmental Change. *BioEssays* 42, e2000004. <https://doi.org/10.1002/bies.202000004>.
115. Sweet, M.J., Croquer, A., and Bythell, J.C. (2011). Bacterial assemblages differ between compartments within the coral holobiont. *Coral Reefs* 30, 39–52. <https://doi.org/10.1007/s00338-010-0695-1>.

116. Ricci, F., Tandon, K., Moßhammer, M., Cho, E.H.-J., Blackall, L.L., Kühn, M., and Verbruggen, H. (2023). Fine-scale mapping of physicochemical and microbial landscapes of the coral skeleton. *Environ. Microbiol.* 25, 1505–1521. <https://doi.org/10.1111/1462-2920.16369>.
117. Cárdenas, A., Raina, J.-B., Pogoreutz, C., Rådecker, N., Bougoure, J., Guagliardo, P., Pernice, M., and Voolstra, C.R. (2022). Greater functional diversity and redundancy of coral endolithic microbiomes align with lower coral bleaching susceptibility. *ISME J.* 16, 2406–2420. <https://doi.org/10.1038/s41396-022-01283-y>.
118. Pollock, F.J., McMinds, R., Smith, S., Bourne, D.G., Willis, B.L., Medina, M., Thurber, R.V., and Zaneveld, J.R. (2018). Coral-associated bacteria demonstrate phylosymbiosis and cophylogeny. *Nat. Commun.* 9, 4921. <https://doi.org/10.1038/s41467-018-07275-x>.
119. Poquita-Du, R.C., Goh, Y.L., Huang, D., Chou, L.M., and Todd, P.A. (2020). Gene Expression and Photophysiological Changes in *Pocillopora acuta* Coral Holobiont Following Heat Stress and Recovery. *Microorganisms* 8, 8. <https://doi.org/10.3390/microorganisms8081227>.
120. Nielsen, J.J.V., Matthews, G., Frith, K.R., Harrison, H.B., Marzoni, M.R., Slaughter, K.L., Suggett, D.J., and Bay, L.K. (2022). Experimental considerations of acute heat stress assays to quantify coral thermal tolerance. *Sci. Rep.* 12, 16831. <https://doi.org/10.1038/s41598-022-20138-2>.
121. Blanckaert, A.C.A., de Barros Marangoni, L.F., Rottier, C., Grover, R., and Ferrier-Pagès, C. (2021). Low levels of ultra-violet radiation mitigate the deleterious effects of nitrate and thermal stress on coral photosynthesis. *Mar. Pollut. Bull.* 167, 112257. <https://doi.org/10.1016/j.marpollbul.2021.112257>.
122. Lohr, K.E., Khattri, R.B., Guingab-Cagmat, J., Camp, E.F., Merritt, M.E., Garrett, T.J., and Patterson, J.T. (2019). Metabolomic profiles differ among unique genotypes of a threatened Caribbean coral. *Sci. Rep.* 9, 6067. <https://doi.org/10.1038/s41598-019-42434-0>.
123. Hackerott, S., Viridis, F., Flood, P.J., Souto, D.G., Paez, W., and Eirin-Lopez, J.M. (2023). Relationships between phenotypic plasticity and epigenetic variation in two Caribbean *Acropora* corals. *Mol. Ecol.* 32, 4814–4828. <https://doi.org/10.1111/mec.17072>.
124. Mayfield, A.B., Chen, Y.-J., Lu, C.-Y., and Chen, C.-S. (2018). The proteomic response of the reef coral *Pocillopora acuta* to experimentally elevated temperatures. *PLoS One* 13, e0192001. <https://doi.org/10.1371/journal.pone.0192001>.
125. Huffmyer, A.S., Bean, N.K., Majerová, E., Harris, C.I., and Drury, C. (2023). Variable intraspecific genetic diversity effects impact thermal tolerance in a reef-building coral. *Coral Reefs* 42, 119–129. <https://doi.org/10.1007/s00338-022-02320-0>.
126. Baker, A.C., Starger, C.J., McClanahan, T.R., and Glynn, P.W. (2004). Coral reefs: Corals' adaptive response to climate change. *Nature* 430, 7001. <https://doi.org/10.1038/430741a>.
127. Glynn, P.W. (1990). Coral Mortality and Disturbances to Coral Reefs in the Tropical Eastern Pacific. In *Elsevier Oceanography Series*, 52, P.W. Glynn, ed. (Elsevier), pp. 55–126. [https://doi.org/10.1016/S0422-9894\(08\)70033-3](https://doi.org/10.1016/S0422-9894(08)70033-3).
128. Glynn, P.W., and D'Croz, L. (1990). Experimental evidence for high temperature stress as the cause of El Niño-coincident coral mortality. *Coral Reefs* 8, 181–191. <https://doi.org/10.1007/BF00265009>.
129. Maté, J.L. (2003). Corals and coral reefs of the Pacific coast of Panamá. In *Latin American Coral Reefs*, J. Cortés, ed. (Elsevier Science), pp. 387–417. <https://doi.org/10.1016/B978-044451388-5/50018-7>.
130. Cuning, R., Glynn, P.W., and Baker, A.C. (2013). Flexible associations between *Pocillopora* corals and *Symbiodinium* limit utility of symbiosis ecology in defining species. *Coral Reefs* 32, 795–801. <https://doi.org/10.1007/s00338-013-1036-y>.
131. Combosch, D.J., and Vollmer, S.V. (2011). Population Genetics of an Ecosystem-Defining Reef Coral *Pocillopora damicornis* in the Tropical Eastern Pacific. *PLoS One* 6, e21200. <https://doi.org/10.1371/journal.pone.0021200>.
132. Toth, L.T., Aronson, R.B., Vollmer, S.V., Hobbs, J.W., Urrego, D.H., Cheng, H., Enochs, I.C., Combosch, D.J., van van Woeseik, R., and Macintyre, I.G. (2012). ENSO Drove 2500-Year Collapse of Eastern Pacific Coral Reefs. *Science* 337, 81–84. <https://doi.org/10.1126/science.1221168>.
133. Cuning, R., Bay, R.A., Gillette, P., Baker, A.C., and Traylor-Knowles, N. (2018). Comparative analysis of the *Pocillopora damicornis* genome highlights role of immune system in coral evolution. *Sci. Rep.* 8, 16134. <https://doi.org/10.1038/s41598-018-34459-8>.
134. Liu, G., Heron, S., Eakin, C., Muller-Karger, F., Vega-Rodriguez, M., Guild, L., De La Cour, J., Geiger, E., Skirving, W., Burgess, T., et al. (2014). Reef-Scale Thermal Stress Monitoring of Coral Ecosystems: New 5-km Global Products from NOAA Coral Reef Watch. *Remote Sens.* 6, 11579–11606. <https://doi.org/10.3390/rs6111579>.
135. Perez, G., Barber, G.P., Benet-Pages, A., Casper, J., Clawson, H., Diekhans, M., Fischer, C., Gonzalez, J.N., Hinrichs, A.S., Lee, C.M., et al. (2025). The UCSC Genome Browser database: 2025 update. *Nucleic Acids Res.* 53, D1243–D1249. <https://doi.org/10.1093/nar/gkae974>.
136. Hume, B.C.C., Smith, E.G., Ziegler, M., Warrington, H.J.M., Burt, J.A., LaJeunesse, T.C., Wiedenmann, J., and Voolstra, C.R. (2019). SymPortal: A novel analytical framework and platform for coral algal symbiont next-generation sequencing ITS2 profiling. *Mol. Ecol. Resour.* 19, 1063–1080. <https://doi.org/10.1111/1755-0998.13004>.
137. McLaren, M.R., and Callahan, B.J. (2021). Silva 138.1 prokaryotic SSU taxonomic training data formatted for DADA2. Zenodo. Version v1. <https://doi.org/10.5281/zenodo.4587955>.
138. Pochon, X., Pawlowski, J., Zaninetti, L., and Rowan, R. (2001). High genetic diversity and relative specificity among *Symbiodinium*-like endosymbiotic dinoflagellates in soritid foraminiferans. *Mar. Biol.* 139, 1069–1078. <https://doi.org/10.1007/s002270100674>.
139. Stat, M., Pochon, X., Cowie, R.O.M., and Gates, R.D. (2009). Specificity in communities of *Symbiodinium* in corals from Johnston Atoll. *Mar. Ecol. Prog. Ser.* 386, 83–96. <https://doi.org/10.3354/meps08080>.
140. Ul-Hasan, S., Bowers, R.M., Figueroa-Montiel, A., Licea-Navarro, A.F., Beman, J.M., Woyke, T., and Nobile, C.J. (2019). Community ecology across bacteria, archaea and microbial eukaryotes in the sediment and seawater of coastal Puerto Nuevo, Baja California. *PLoS One* 14, e0212355. <https://doi.org/10.1371/journal.pone.0212355>.
141. Parada, A.E., Needham, D.M., and Fuhrman, J.A. (2016). Every base matters: Assessing small subunit rRNA primers for marine microbiomes with mock communities, time series and global field samples. *Environ. Microbiol.* 18, 1403–1414. <https://doi.org/10.1111/1462-2920.13023>.
142. Apprill, A., McNally, S., Parsons, R., and Weber, L. (2015). Minor revision to V4 region SSU rRNA 806R gene primer greatly increases detection of SAR11 bacterioplankton. *Aquat. Microb. Ecol.* 75, 129–137. <https://doi.org/10.3354/ame01753>.
143. Bourgey, M., Dali, R., Eveleigh, R., Chen, K.C., Letourneau, L., Fillon, J., Michaud, M., Caron, M., Sandoval, J., Lefebvre, F., et al. (2019). GenPipes: An open-source framework for distributed and scalable genomic analyses. *GigaScience* 8, giz037. <https://doi.org/10.1093/giga-science/giz037>.
144. Burrows, M., and Wheeler, D.J. (1994). A block-sorting lossless data compression algorithm. *SRS Research Report*, 124. https://www.cs.jhu.edu/~langmea/resources/burrows_wheeler.pdf.
145. McKenna, A.H., Hanna, M., Banks, E., Sivachenko, A., Cibulskis, K., Kernytzky, A., Garimella, K., Altshuler, D., Gabriel, S., Daly, M., et al. (2010). The Genome Analysis Toolkit: A MapReduce framework for analyzing next-generation DNA sequencing data. *Genome Res.* 20, 1297–1303. <https://doi.org/10.1101/gr.107524.110>.
146. Danecek, P., Auton, A., Abecasis, G., Albers, C.A., Banks, E., DePristo, M.A., Handsaker, R.E., Lunter, G., Marth, G.T., Sherry, S.T., et al. (2011). The variant call format and VCFtools. *Bioinformatics* 27, 2156–2158. <https://doi.org/10.1093/bioinformatics/btr330>.

147. Purcell, S., Neale, B., Todd-Brown, K., Thomas, L., Ferreira, M.A.R., Bender, D., Maller, J., Sklar, P., De Bakker, P.I.W., Daly, M.J., et al. (2007). PLINK: A Tool Set for Whole-Genome Association and Population-Based Linkage Analyses. *Am. J. Hum. Genet.* *81*, 559–575. <https://doi.org/10.1086/519795>.
148. Goudet, J. (2005). HIERFSTAT, a package for R to compute and test hierarchical *F*-statistics. *Mol. Ecol. Notes* *5*, 184–186. <https://doi.org/10.1111/j.1471-8286.2004.00828.x>.
149. Luu, K., Bazin, E., and Blum, M.G.B. (2017). pcadapt: An R package to perform genome scans for selection based on principal component analysis. *Mol. Ecol. Resour.* *17*, 67–77. <https://doi.org/10.1111/1755-0998.12592>.
150. Whitlock, M.C., and Lotterhos, K.E. (2015). Reliable Detection of Loci Responsible for Local Adaptation: Inference of a Null Model through Trimming the Distribution of *F*(ST). *Am. Nat.* *186*, S24–S36. <https://doi.org/10.1086/682949>.
151. Cingolani, P., Platts, A., Wang, L.L., Coon, M., Nguyen, T., Wang, L., Land, S.J., Lu, X., and Ruden, D.M. (2012). A program for annotating and predicting the effects of single nucleotide polymorphisms, SnpEff: SNPs in the genome of *Drosophila melanogaster* strain w¹¹¹⁸; iso-2; iso-3. *Fly* *6*, 80–92. <https://doi.org/10.4161/fly.19695>.
152. Chen, Y., Ye, W., Zhang, Y., and Xu, Y. (2015). High speed BLASTN: An accelerated MegaBLAST search tool. *Nucleic Acids Res.* *43*, 7762–7768. <https://doi.org/10.1093/nar/gkv784>.
153. Pinheiro, J.C., and Bates, D.M. (1996). Unconstrained parametrizations for variance-covariance matrices. *Stat. Comput.* *6*, 289–296. <https://doi.org/10.1007/BF00140873>.
154. Lindstrom, M.L., and Bates, D.M. (1990). Nonlinear Mixed Effects Models for Repeated Measures Data. *Biometrics* *46*, 673–687. <https://doi.org/10.2307/2532087>.
155. McMurdie, P.J., and Holmes, S. (2013). phyloseq: An R Package for Reproducible Interactive Analysis and Graphics of Microbiome Census Data. *PLoS One* *8*, e61217. <https://doi.org/10.1371/journal.pone.0061217>.
156. Dixon, P. (2003). VEGAN, a package of R functions for community ecology. *J. Veg. Sci.* *14*, 927–930. <https://doi.org/10.1111/j.1654-1103.2003.tb02228.x>.
157. Martínez Arbizu, P. (2020). pairwiseAdonis: Pairwise multilevel comparison using adonis. R package version 0.4. <https://github.com/pmartinezarbizu/pairwiseAdonis>.
158. De Cáceres, M.D., and Legendre, P. (2009). Associations between species and groups of sites: Indices and statistical inference. *Ecology* *90*, 3566–3574. <https://doi.org/10.1890/08-1823.1>.
159. Callahan, B.J., McMurdie, P.J., Rosen, M.J., Han, A.W., Johnson, A.J.A., and Holmes, S.P. (2016). DADA2: High-resolution sample inference from Illumina amplicon data. *Nat. Methods* *13*, 7. <https://doi.org/10.1038/nmeth.3869>.
160. Martin, M. (2011). Cutadapt removes adapter sequences from high-throughput sequencing reads. *EMBnet.j.* *17*, 1. <https://doi.org/10.14806/ej.17.1.200>.
161. Love, M.I., Huber, W., and Anders, S. (2014). Moderated estimation of fold change and dispersion for RNA-seq data with DESeq2. *Genome Biol.* *15*, 550. <https://doi.org/10.1186/s13059-014-0550-8>.
162. Broad Institute (2019). Picard Toolkit (Broad Institute). GitHub Repository. <https://broadinstitute.github.io/picard/>.
163. Connelly, M.T., Snyder, G., Palacio-Castro, A.M., Gillette, P.R., Baker, A. C., and Traylor-Knowles, N. (2023). Antibiotics reduce *Pocillopora* coral-associated bacteria diversity, decrease holobiont oxygen consumption and activate immune gene expression. *Mol. Ecol.* *32*, 4677–4694. <https://doi.org/10.1111/mec.17049>.
164. Johnston, E.C., Forsman, Z.H., Flot, J.-F., Schmidt-Roach, S., Pinzón, J. H., Knapp, I.S.S., and Toonen, R.J. (2017). A genomic glance through the fog of plasticity and diversification in *Pocillopora*. *Sci. Rep.* *7*, 5991. <https://doi.org/10.1038/s41598-017-06085-3>.
165. Flot, J.-F., and Tillier, S. (2007). The mitochondrial genome of *Pocillopora* (Cnidaria: Scleractinia) contains two variable regions: The putative D-loop and a novel ORF of unknown function. *Gene* *401*, 80–87. <https://doi.org/10.1016/j.gene.2007.07.006>.
166. Gélin, P., Postaire, B., Fauvelot, C., and Magalon, H. (2017). Reevaluating species number, distribution and endemism of the coral genus *Pocillopora* Lamarck, 1816 using species delimitation methods and microsatellites. *Mol. Phylogenet. Evol.* *109*, 430–446. <https://doi.org/10.1016/j.ympev.2017.01.018>.
167. Oury, N., Noël, C., Mona, S., Aurelle, D., and Magalon, H. (2023). From genomics to integrative species delimitation? The case study of the Indo-Pacific *Pocillopora* corals. *Mol. Phylogenet. Evol.* *184*, 107803. <https://doi.org/10.1016/j.ympev.2023.107803>.
168. R Core Team (2022). R: A Language and Environment for Statistical Computing (R Foundation for Statistical Computing). <https://www.R-project.org/>.
169. Carbeck, K., Arcese, P., Lovette, I., Pruett, C., Winker, K., and Walsh, J. (2023). Candidate genes under selection in song sparrows co-vary with climate and body mass in support of Bergmann’s Rule. *Nat. Commun.* *14*, 6974. <https://doi.org/10.1038/s41467-023-42786-2>.
170. Stronen, A.V., Pertoldi, C., Iacolina, L., Kadarmideen, H.N., and Kristensen, T.N. (2019). Genomic analyses suggest adaptive differentiation of northern European native cattle breeds. *Evol. Appl.* *12*, 1096–1113. <https://doi.org/10.1111/eva.12783>.
171. Shogren, E.H., Sardell, J.M., Muirhead, C.A., Martí, E., Cooper, E.A., Moyle, R.G., Presgraves, D.C., and Uy, J.A.C. (2024). Recent secondary contact, genome-wide admixture, and asymmetric introgression of neo-sex chromosomes between two Pacific island bird species. *PLoS Genet.* *20*, e1011360. <https://doi.org/10.1371/journal.pgen.1011360>.
172. Sandercock, A.M., Westbrook, J.W., Zhang, Q., Johnson, H.A., Saielli, T. M., Scivani, J.A., Fitzsimmons, S.F., Collins, K., Perkins, M.T., Craddock, J.H., et al. (2022). Frozen in time: Ranges-wide genomic diversity, structure, and demographic history of relict American chestnut populations. *Mol. Ecol.* *31*, 4640–4655. <https://doi.org/10.1111/mec.16629>.
173. National Center for Biotechnology Information. (2024). NCBI *Pocillopora damicornis* Annotation Release 100. RefSeq. https://www.ncbi.nlm.nih.gov/refseq/annotation_euk/Pocillopora_damicornis/100/.
174. Hoogenboom, M., Beraud, E., and Ferrier-Pagès, C. (2010). Relationship between symbiont density and photosynthetic carbon acquisition in the temperate coral *Cladocora caespitosa*. *Coral Reefs* *29*, 21–29. <https://doi.org/10.1007/s00338-009-0558-9>.
175. Schmidt, C., Heinz, P., Kucera, M., and Uthicke, S. (2011). Temperature-induced stress leads to bleaching in larger benthic foraminifera hosting endosymbiotic diatoms. *Limnol. Oceanogr.* *56*, 1587–1602. <https://doi.org/10.4319/lo.2011.56.5.1587>.
176. Bradford, M.M. (1976). A rapid and sensitive method for the quantitation of microgram quantities of protein utilizing the principle of protein-dye binding. *Anal. Biochem.* *72*, 248–254. [https://doi.org/10.1016/0003-2697\(76\)90527-3](https://doi.org/10.1016/0003-2697(76)90527-3).
177. Veal, C.J., Carmi, M., Fine, M., and Hoegh-Guldberg, O. (2010). Increasing the accuracy of surface area estimation using single wax dipping of coral fragments. *Coral Reefs* *29*, 893–897. <https://doi.org/10.1007/s00338-010-0647-9>.
178. Lesser, M.P. (2006). OXIDATIVE STRESS IN MARINE ENVIRONMENTS: Biochemistry and Physiological Ecology. *Annu. Rev. Physiol.* *68*, 253–278. <https://doi.org/10.1146/annurev.physiol.68.040104.110001>.
179. Huang, D., Ou, B., and Prior, R.L. (2005). The Chemistry behind Antioxidant Capacity Assays. *J. Agric. Food Chem.* *53*, 1841–1856. <https://doi.org/10.1021/jf030723c>.
180. Bray, J.R., and Curtis, J.T. (1957). An Ordination of the Upland Forest Communities of Southern Wisconsin. *Ecol. Monogr.* *27*, 325–349. <https://doi.org/10.2307/1942268>.
181. Dufréne, M., and Legendre, P. (1997). Species Assemblages and Indicator Species: The Need for a Flexible Asymmetrical Approach.

- Ecol. Monogr. 67, 345–366. [https://doi.org/10.1890/0012-9615\(1997\)067\[0345:SAAIST\]2.0.CO;2](https://doi.org/10.1890/0012-9615(1997)067[0345:SAAIST]2.0.CO;2).
182. Quast, C., Pruesse, E., Yilmaz, P., Gerken, J., Schweer, T., Yarza, P., Peplies, J., and Glöckner, F.O. (2013). The SILVA ribosomal RNA gene database project: Improved data processing and web-based tools. *Nucleic Acids Res.* 41, D590–D596. <https://doi.org/10.1093/nar/gks1219>.
183. Davis, N.M., Proctor, D.M., Holmes, S.P., Relman, D.A., and Callahan, B. J. (2018). Simple statistical identification and removal of contaminant sequences in marker-gene and metagenomics data. *Microbiome* 6, 226. <https://doi.org/10.1186/s40168-018-0605-2>.
184. Evensen, N.R., Voolstra, C.R., Fine, M., Perna, G., Buitrago-López, C., Cárdenas, A., Banc-Prandi, G., Rowe, K., and Barshis, D.J. (2022). Empirically derived thermal thresholds of four coral species along the Red Sea using a portable and standardized experimental approach. *Coral Reefs* 41, 239–252. <https://doi.org/10.1007/s00338-022-02233-y>.
185. Zuur, A.F., Ieno, E.N., Walker, N.J., Saveliev, A.A., and Smith, G.M. (2009). *Mixed Effects Models and Extensions in Ecology with R* 574 (Springer), p. 574.

STAR★METHODS

KEY RESOURCES TABLE

REAGENT or RESOURCE	SOURCE	IDENTIFIER
Chemicals, peptides, and recombinant proteins		
DNA/RNA Shield	Zymo Research	Cat#R1100-250
Ethyl alcohol	Millipore Sigma	Cat#1590102500
Lysing Matrix A, bulk, 200 g	MP Biomedicals	Cat#116540423
Ceramic Spheres, 6.35 mm (1/4"), bulk	MP Biomedicals	Cat#116540424-CF
Proteinase K, recombinant, PCR grade	Thermo Scientific	Cat#EO0491
RNase A (17,500 U)	Qiagen	Cat#19101
UltraPure™ Phenol:Chloroform: Isoamyl Alcohol (25:24:1, v/v)	Invitrogen	Cat#15593049
Chloroform:Isoamyl alcohol 24:1	Millipore Sigma	Cat#C0549-1QT
Sodium Acetate Solution (3 M), pH 5.2	Thermo Scientific	Cat#R1181
2-Propanol	Millipore Sigma	Cat#909955-500ML
UltraPure™ DNase/RNase-Free Distilled Water	Invitrogen	Cat#10977015
Pierce™ Bovine Serum Albumin Standard Ampules, 2 mg/mL	Thermo Scientific	Cat#23209
Critical commercial assays		
Pierce™ Bradford Protein Assay Kit	Thermo Scientific	Cat#23200
TBARS (TCA Method) Assay Kit	Cayman Chemical	Cat#700870
OxiSelect™ TAC Assay Kit	Cell Biolabs Inc.	Cat#STA-360
Deposited data		
All whole genome and marker-gene [internal transcribed spacer 2 (ITS2) and 16S] data used for the analyses	This paper, available on NCBI	NCBI BioProject: PRJNA1134702
All mtORF data used for the analyses	This paper, available on NCBI	NCBI BioProject: PRJNA1135493
All physiology and oxidative metabolism data used for the analyses	This paper, available on Zenodo	https://doi.org/10.5281/zenodo.15532242
<i>Pocillopora damicornis</i> reference genome and assembly	Cunning et al. ¹³³	NCBI BioProject: PRJNA454489
<i>Pocillopora damicornis</i> RefSeq Genome sequencing and assembly	RefSeq	NCBI BioProject: PRJNA506040
NOAA Daily Global 5km Satellite Coral Bleaching Heat Stress Monitoring	Liu et al. ¹³⁴	https://coralreefwatch.noaa.gov/product/5km/
UCSC Genome Browser	Perez et al. ¹³⁵	https://genome.ucsc.edu/
SymPortal	Hume et al. ¹³⁶	https://symportal.org/
Silva 138.1 prokaryotic SSU taxonomic training data formatted for DADA2	McLaren et al. ¹³⁷	https://doi.org/10.5281/zenodo.4587955
Oligonucleotides		
ITS2 primers for Symbiodiniaceae, ITS-DINO and ITS2Rev2; F: 5'-GTGAATTGCAGAACTCCGTG-3', R: 5'-CCTCGCTTACTTATATGCTT-3'	Pochon et al. ¹³⁸ ; Stat et al. ¹³⁹	N/A
Earth Microbiome Project's updated 16S primers 515F and 806R; F: 5'-GTGYCAGCMGCCGCGGTAA-3', R: 5'-GGACTACNVGGGTWTCTAAT-3'	Ul-Hasan et al. ¹⁴⁰ ; Parada et al. ¹⁴¹ ; Apprill et al. ¹⁴²	N/A
Software and algorithms		
GenPipes	Bourgey et al. ¹⁴³	https://doi.org/10.1093/gigascience/giz037

(Continued on next page)

Continued

REAGENT or RESOURCE	SOURCE	IDENTIFIER
Picard	Broad Institute	https://broadinstitute.github.io/picard/ ; RRID:SCR_006525
BWA	Burrows and Wheeler ¹⁴⁴	N/A
GATK Haplotype Caller	McKenna et al. ¹⁴⁵	https://gatk.broadinstitute.org/hc/en-us
VCFTools	Danecek et al. ¹⁴⁶	https://vcftools.github.io/index.html
PLINK	Purcell et al. ¹⁴⁷	https://github.com/chrchang/plink-ng
ADMIXTURE	Alexander and Lange ⁸²	https://dalexander.github.io/admixture/
hierstat	Goudet ¹⁴⁸	https://github.com/jgx65/hierstat
pcadapt	Luu et al. ¹⁴⁹	https://bcm-uga.github.io/pcadapt/
OutFLANK	Whitlock and Lotterhos ¹⁵⁰	https://github.com/whitlock/OutFLANK
snpEff	Cingolani et al. ¹⁵¹	https://pcingola.github.io/SnpEff/
BLAST	Chen et al. ¹⁵²	https://blast.ncbi.nlm.nih.gov/Blast.cgi
R version 4.2.1	R Core Team	https://cran.rstudio.com/
nlme	Pinheiro and Bates ¹⁵³ ; Lindstrom and Bates ¹⁵⁴	https://cran.r-project.org/web/packages/nlme/index.html
phyloseq	McMurdie and Holmes ¹⁵⁵	https://doi.org/10.1371/journal.pone.0061217
vegan	Dixon ¹⁵⁶	https://github.com/vegandevs/vegan
pairwise.adonis	Martinez Arbizu ¹⁵⁷	https://github.com/pmartinezarbizu/pairwiseAdonis
indicspecies	Cáceres and Legendre ¹⁵⁸	https://emf-creaf.github.io/indicspecies/
'DADA2' version 1.20	Callahan et al. ¹⁵⁹	https://benjjneb.github.io/dada2/
cutadapt	Martin ¹⁶⁰	https://cutadapt.readthedocs.io/en/stable/
DESeq2	Love et al. ¹⁶¹	https://github.com/theislab/DESeq2
Other		
200 W titanium heaters	Schego	Cat#546
NovaTec IceProbe Small Aquarium Chillers	Bulk Reef Supply	SKU#208272
Arduino Mega 2560	Arduino	SKU#A000067
Roleadro Led Aquarium Light, Dimmable Coral Reef Light 165W for Fish Tank, Full Spectrum Grow Suitable 55-75 Gallon Freshwater and Saltwater Galaxyhydro	Amazon	N/A
Sun Sun JVP-110 528-Gph Wave Maker Pumps	Amazon	N/A
Jecod/Jebao DCT Marine Controllable Water Pump (DCT-4000, 1056GPH)	Amazon	N/A
HOBO Pendant Temperature/Light 64K Data Logger	HOBO	Part#UA-002-64

EXPERIMENTAL MODEL AND STUDY PARTICIPANT DETAILS

To explore how the upwelling regime in Panama's Tropical Eastern Pacific (TEP) influences *Pocillopora* corals' holobiont configurations and their functional consequences, we used both observational and experimental approaches to determine how coral-microbiome interactions were impacting thermotolerance. Specifically, we investigated how the TEP's seasonal upwelling regime impacts population genetic structure, microbiome dynamics, and holobiont physiological and biochemical pathways during an acute thermal stress assay. To quantify genetic differentiation across the TEP and ascertain potential local adaptation to upwelling regimes, we conducted whole-genome shallow shotgun sequencing of coral colonies across the Gulf of Panama and the Gulf of Chiriquí. To determine whether and how different holobiont configurations were associated with thermotolerance, we ran an acute thermal stress assay known as the Coral Bleaching Automated Stress System (CBASS; following Voolstra et al.⁶⁴) which subjected corals to a range of experimentally manipulated temperatures. Specifically, to determine algal and prokaryotic community dynamics during the CBASS experiments, we sequenced ITS2 and 16S marker genes, respectively. To assess differences in host physiological responses between upwelling regimes, we tested for differences between gulfs in their functional responses of host tissue protein and chlorophyll *a* concentrations to increasing temperatures. Lastly, to determine how the oxidative metabolism of the coral holobiont is

impacted by upwelling, we quantified how total antioxidant capacity and lipid peroxidation vary as a function of temperature for each gulf. All corals were collected under permits issued by the Panamanian Ministry of the Environment (permit reference numbers SE/AO-4-19, ARB/ARG-093-2022, and ARB/ARG-090-2022). All scripts used in our analyses, alongside the physiology and oxidative metabolism data can be found at <https://doi.org/10.5281/zenodo.15532242>. All generated sequence data is available on the NCBI Sequence Read Archive (SRA) under NCBI BioProject PRJNA1134702 and PRJNA1135493.

Field collections

In November–December 2020, we permanently marked 11–12 coral colonies in six different reef sites across Panama’s Tropical Eastern Pacific. Three of these reefs were located in the Gulf of Panama, and the other three were located in the Gulf of Chiriquí. Colonies were selected as discernibly distinct coral colonies within 3–5 meters of a 50 m transect. Using Self Contained Underwater Breathing Apparatuses (SCUBA), we hammered into the reef matrix three PVC pipes to mark each colony, with a unique plastic cow tag attached at the end of one of them. We sampled these tagged corals for both population genetic analyses and our acute heat stress experiment. For the acute heat stress experiment, we collected 8 different coral branches from each colony, one for each of the temperature treatments. These were collected with SCUBA and removed using stainless steel bone cutters. Gloves were worn during the collection process. We selected branches approximately 10–12 cm long, and at least 2 cm in diameter. For the host population genetic analyses, we only collected a single branch, following the same protocol described above. This branch was further fragmented and placed into a 15 mL tube with 10 mL of DNA/RNA Shield (Zymo Research). We disinfected the bone cutters with >95% ethanol and wiped them with a clean Kimwipe in between coral colonies. We stored collected samples at 4°C for the duration of the field work, and then placed them at –80°C for long term storage prior to analyses.

METHOD DETAILS

Host population genetics

To determine the genetic landscape of corals across Panama’s Tropical Eastern Pacific, we extracted DNA from each in-situ sample using a modified phenol–chloroform protocol we optimized for corals. Briefly, we first lysed the coral branch, tissue, and skeleton together in DNA/RNA Shield (Zymo Research) using a combination of Lysing Matrix A and 1/4-inch ceramic spheres (MP Biomedicals). This was followed by enzymatic digestion using both proteinase K and RNAse A, and a standard phenol:chloroform:isoamyl phase separation. This protocol allowed for the production of high quantity and high molecular weight DNA. The resulting DNA was shipped to the McGill Genome Center (Montréal, Québec) where we performed shallow whole genome sequencing for all our coral samples. We aimed for 4M reads per sample with a pair-end read length of 150 bp. The center performed the library preparation and sequenced all samples on a single lane of an Illumina NovaSeq6000 S-Prime v1.5. The colony-region breakdown for analyzed samples can be found in [Data S3A](#).

SNP-by-genotyping

To determine the genetic variation across our samples, we used SNP-by-genotyping with GenPipes¹⁴³ on the Digital Research Alliance of Canada’s high-performance computing (HPC) cluster. We implemented quality control and SNP filtering steps to align trimmed reads to our reference genome,¹⁴⁴ Picard to mark fragment duplicates¹⁶² (<https://broadinstitute.github.io/picard/>), and the GATK Haplotype Caller¹⁴⁵ to call SNPs. We used the *Pocillopora damicornis* coral genome as a reference genome.¹³³ Although recent work has determined that corals in Panama’s Tropical Eastern Pacific are not *P. damicornis* as previously believed, but part of the *P. verrucosa*–*P. grandis*/*P. meandrina* complex,^{26,163,164} the genome assembled by Cunning et al.¹³³ was generated from an individual located in a plot adjacent to our Saboga reef transect in the Gulf of Panama; the *P. damicornis* reference genome on NCBI thus most likely forms part of the *P. verrucosa*–*P. grandis*/*P. meandrina* lineages and is an appropriate reference genome for this work. To determine the genetic lineages of our colonies, we amplified and Sanger sequenced the mitochondrial Open Reading Frame (mtORF), following Flot and Tiller¹⁶⁵ and Gélin et al.¹⁶⁶ Amplifying the mtORF is currently the most commonly implemented technique to distinguish between different *Pocillopora* spp. lineages (see Oury et al.¹⁶⁷). Hereon, genetic lineages will be referred to by their mtORF lineage. We were unable to amplify the mtORF for two colonies, 755 in UVA and 713 in SAB. These two colonies have been removed from downstream population genetic analyses that consider trends across mtORF lineages.

Prior to population genetic analyses, we engaged in quality control filtering using VCFtools,¹⁴⁶ and pruned loci potentially under linkage disequilibrium using PLINK.¹⁴⁷ All statistical analyses were performed in R version 4.2.1.¹⁶⁸ After filtering, we retained 6,145 SNPs for downstream analyses. To determine the contribution of different ancestral source populations within our samples, we ran the program ADMIXTURE.⁸² To determine the optimal number of K ancestral populations, we used ADMIXTURE’s cross-validation (CV) error plot (see [Figure S1](#)). For regional analyses, given the equivalence in the CV error values for K= 3, 4, 5, and 6, we selected K = 6 among the K values because this number allows us to test our a priori expectation that each reef site if each site represents a distinct ancestral lineage.^{82,169–172} Using K = 3 to 5 does not yield materially different conclusions, which is that there is notable gene flow across our six reef sites, but would not allow us to investigate differences between sites ([Figure S1A](#)). Plots for K= 3 to 5 can be accessed and generated from our scripts on Zenodo (<https://doi.org/10.5281/zenodo.15532242>). For mtORF analyses, we selected K = 4 as it had the smallest CV error value (see [Figure S1B](#)).

Genetic differentiation metrics

To determine genetic differentiation metrics across all samples, we used the command ‘basic.stats’ from the package ‘hierfstat’¹⁴⁸ in R version 4.2.1.¹⁶⁸ For pairwise F_{st} calculations, we used the command ‘genet.dist’ with the Weir and Cockerham 1984 calculation from the package ‘hierfstat’.¹⁴⁸ To detect genetic markers involved in adaptation to contrasting upwelling regimes, we implemented the program ‘pcadapt’.¹⁴⁹ We used the principal component analysis approach in ‘pcadapt’ as it can handle admixed individuals and does not require pre-grouping individuals, while also implementing the robust Mahalanobis distance that can account for potential outlier loci.¹⁴⁹ As our population genetic analyses suggest that mtORF lineages are not completely isolated, with some individuals showing mixed ancestry, we ran outlier analyses for both lineages together (see Figure S2). To detect putative outlier loci that may be underlying the adaptation to different gulfs, we implemented the package ‘OutFLANK’.¹⁵⁰ We chose to use ‘OutFLANK’ as it defines a null F_{st} distribution based on expected genomic signatures of diversifying and balancing selection. This program identifies loci under divergent selection by comparing the allele frequencies between populations, in our case the two studied gulfs. To account for F_{st} outliers driven by within-gulf microhabitat adaptation, we re-ran ‘OutFLANK’ setting each reef as the population, as compared to setting each population as one of the two regions (Gulf of Panama, Gulf of Chiriquí). Any within-gulf outliers detected in our reef-based ‘OutFLANK’ analysis were filtered from downstream outlier functional analysis. We defined outliers at a q -value cut-off of 0.05 and expected heterozygosity cut-off of 0.1.

Functional predictions of outlier loci

To determine the potential functional roles of the identified outlier loci, we used snpEff¹⁵¹ to annotate and determine the predicted effects of the identified variants. To do so, we built a custom snpEff database, using NCBI’s RefSeq annotation for the *P. damicornis* genome¹⁷³ (https://www.ncbi.nlm.nih.gov/genome/annotation_euk/Pocillopora_damicornis/100/). We selected loci that snpEff denoted as being missense variants and intron variants for further characterization, given these SNP would most strongly impact downstream proteins. We defined a 2000 kb window around each of these SNPs using the UCSC Genome Browser.¹³⁵ We then inputted this window into nucleotide BLAST (blastn) and compared our genomic windows to the nucleotide collection¹⁵² to predict the associated proteins containing outlier SNPs; we selected the resulting hit with the highest percent identity.

Acute thermal stress assay

To test the functional consequences of *Pocillopora* coral’s host-microbiome interactions, we subjected all sampled corals to the Coral Bleaching Automated Stress System (CBASS). We selected this assay as it has been shown to correlate with thermal tolerance trends, ranging from microbiome dynamics to host physiological shifts, as detected from traditional, multi-week heat stress experiments.^{64,104} Following Voolstra et al.⁶⁴, we used eight, 10 L flow-through tanks representing independently controlled temperature treatments. Each tank’s temperature was regulated by 200 W titanium heaters (Schego) and IceProbe Small Aquarium Chillers (Nova Tec), connected to a custom-built controller with a 12V power supply (Arduino Mega 2560). Full spectrum 165W aquarium LED lights (Galaxyhydro) provided ~ 600 mmol quanta $m^{-2} s^{-1}$ to each tank on a 12 h:12 h light:dark cycle. Throughout the experiment, each tank received water at a rate of approximately 2 L hr^{-1} , with powerheads (SUNSUN JVP Series) and a reservoir pump (Jecod/Jebao DCT-4000) ensuring sufficient water flow. We also placed within each tank a HOBO Pendant Temperature Logger to record temperatures throughout the experiment at 5-minute intervals.

We programmed each tank to run one of eight temperature profiles. These temperature profiles represent the mean monthly maximum (MMM) temperature during our sampling period (28.5°C), and 1.5°C increments from the MMM up to MMM + 10.5°C. The 28.5°C tank served as our control and remained at this temperature throughout the experiment at each site. MMM was determined from the NOAA Coral Reef Watch’s 5 km global product¹³⁴ (<https://coralreefwatch.noaa.gov/product/5km/>). Experiments began at 10:00 AM, with a three hour ramp up to temperature, a temperature hold for three hours, and a ramp down to MMM for two hours. For all tanks, there was an overnight hold at MMM. Sampling began at sunrise for all sites, which was approximately 7:00 AM. From each sample, we used bone cutters to cut small pieces of coral fragments and placed them in 1.5 mL of DNA/RNA Shield (Zymo Research) for downstream microbiome analyses. For physiological and oxidative stress analyses, we collected a single intact branch from the same sample which was first placed within a Whirl-Pak bag wrapped in aluminum foil before being stored in a liquid nitrogen dewar. We removed a single site from all downstream analyses, Contadora in the Gulf of Panama, due to poor temperature control for the 28.5°C treatment.

Microbiome characterization

To characterize microbial dynamics during the Coral Bleaching Automated Stress System (CBASS), we performed amplicon sequencing of the coral Symbiodiniaceae and prokaryotic community. We used the same phenol-chloroform protocol described above to extract DNA from the samples collected during the CBASS. We selected a subset of colonies and sites, representing two reefs per region, and four temperature treatments: 28.5°C (control), 30°C, 33°C, and 36°C; the precise sample breakdown can be found in Data S3A. The resulting DNA was amplified for two markers, ITS2 rRNA for the dinoflagellate algal symbionts in the family Symbiodiniaceae and 16S rRNA for the prokaryotic community.

For ITS2 amplification, we used the ITS-DINO (5’-GTGAATTGCAGAACTCCGTG-3’; Pochon et al.¹³⁸) and ITS2Rev2 (5’-CCTCCGCTTACTTATATGCTT-3’; Stat et al.¹³⁹) primer pairs. For 16S, we followed the amplification protocol from the Earth Microbiome Project’s protocol (Ul-Hasan et al.¹⁴⁰; <https://earthmicrobiome.org/protocols-and-standards/16s/>) using their updated 515F (5’-GTGYCAGCMGCCGCGGTAA-3’; Parada et al.¹⁴¹) and 806R (5’-GGACTACNVGGGTWTCTAAT-3’; Apprill et al.¹⁴²) primer pair. Precise PCR conditions can be found in Data S3B and S3C. Library prep was performed at the Naos Marine Laboratories at the

Smithsonian Tropical Research Institute (Panamá, Republic of Panama) and sequenced on an Illumina MiSeq v2, with a pair-end read length of 250 bp.

We identified taxa from ITS2 reads using the SymPortal platform,¹³⁶ as this database is specifically curated for coral-associated Symbiodiniaceae. SymPortal is a community-driven tool that is able to differentiate intra- and inter-genomic sources of genetic variation across Symbiodiniaceae and thus defines putative taxa on the basis of defining intragenomic (ITS2 sequence) variants (DIVs) rather than amplicon sequence variants (ASVs).¹³⁶ The co-occurrence patterns of DIVs are used by SymPortal to predict ITS2 type profiles, thus leveraging ITS2 intragenomic diversity to delineate putative taxa.¹³⁶ We used the ITS2 type profiles to visualize changes in taxa over the course of the Coral Bleaching Automated Stress System across regions and mtORF lineages. For our GLS models, ordination plots, and indicator species analyses, we used the post-MED DIV count table in R version 4.2.1.¹⁶⁸ Here, we used the absolute abundance DIV table as our ASV table in the R package ‘phyloseq’¹⁵⁵ (<https://github.com/joey711/phyloseq>).

Physiological measurements

We extracted chlorophyll *a* and coral host soluble protein content following Hoogenboom et al.¹⁷⁴ with some modifications. Briefly, we extracted coral holobiont tissue from the skeleton and placed this in 15 mL of 0.45 μM filtered sea water (FSW) using an airbrush. The resulting tissue slurry was then homogenized using a potter grinder. We determined chlorophyll *a* concentrations using the method adapted for microplate readers described by Schimidt et al.¹⁷⁵ We centrifuged 2 mL of the homogenized tissue slurry at 8,000 \times g for 10 min, after which the supernatant was discarded and the resulting symbionts were resuspended in 2 mL of 95% ethanol for chlorophyll *a* extraction. We assessed the soluble protein content using the Bradford Protein Assay Kit (Thermo Scientific, USA) following the manufacturer’s instructions which is based on the Bradford method.¹⁷⁶ To determine absorbance measurements we used a microplate reader (Elx 800, Biotek), and normalized data to surface area (cm^2) using the wax-dipping method.¹⁷⁷

Oxidative metabolism measurements

We prepared samples for oxidative metabolism analyses as previously described in Fernandes de Barros Marangoni et al.^{35,38} Briefly, coral fragments (approximately 0.5 cm^2) were homogenized in ice using ultrasound, with specific buffer solutions tailored for each analysis. After homogenization, we centrifuged the holobiont samples at 13,000 \times g and 4°C for 10 minutes. We normalized our results based on the total holobiont protein content in the sample, which was determined using the Bradford Protein Assay Kit (Thermo Scientific, USA). We generated a protein standard curve using a bovine serum albumin (BSA) solution (2 mg/mL).

Lipid peroxidation

To measure oxidative damage to biomolecules, we quantified the amount of lipid peroxidation (LPO) within each sample. LPO is one of the most prevalent mechanisms of cellular injury and has been extensively reported for corals and other marine organisms under oxidative stress.^{35,178} To detect LPO, we used the Thiobarbituric Acid Reactive Substances (TBARS) method with the commercial kit “TBARS (TCA Method) Assay Kit” (Cayman Chemical, No 700870) following the manufacturer’s instructions. The reaction between malondialdehyde (MDA) and Thiobarbituric Acid (TBA) under high temperatures (90–100°C) and acidic conditions creates an MDA-TBA adduct. We performed this reaction within each of our samples, and measured the resulting adduct calorimetrically at 540 nm using a microplate reader (ELx800, Biotek). We normalized our data by considering the total holobiont protein content in each well of the sample homogenates and expressed this as μM MDA mg protein⁻¹. Given the low amounts of holobiont tissue biomass for our LPO samples at 36°C, we only have data for the remaining three temperature treatments, here 28.5°C, 30°C, and 33°C (see [Data S3A](#) for the sample breakdown).

Total antioxidant capacity

To assess each fragment’s non-enzymatic total antioxidant capacity (TAC), we used the “OxiSelect™ TAC Assay Kit” (Cell Biolabs Inc.) following the manufacturer’s guidelines. This assay quantifies TAC through a single electron transfer mechanism,¹⁷⁹ relying on the reduction of copper (II) to copper (I) by antioxidants. Following reduction, copper (I) ions react with a chromogenic reagent, yielding a maximum absorbance at 490 nm. We compared our sample’s absorbance values with a uric acid standard curve, with absorbance directly proportional to the sample’s reductive capacity. We conducted our measurements using a microplate reader (Elx-800, Biotek), and normalized our data based on the total holobiont protein content in each well of the sample homogenates, expressed as μM Copper Reducing Equivalents (CRE) mg protein⁻¹. For these analyses, we selected four separate temperature treatments: 28.5°C, 30°C, 33°C and 36°C (see [Data S3A](#) for the sample breakdown). These temperatures were selected based on our preliminary microbiome and physiology analyses, which suggested that the thermal threshold for corals in both regions was located within this range (see [Results](#)).

QUANTIFICATION AND STATISTICAL ANALYSES

Microbiome characterization

Symbiodiniaceae

To test the factors significantly driving the observed algal microbiome trends, we modeled the relative proportion of ITS sub-clades as a function of temperature treatment, region, and mtORF as explanatory variables, using the generalized least squares (GLS) function ‘gls’¹⁵³ from the ‘nlme’¹⁵⁴ package in R version 4.2.1.¹⁶⁸ We used GLS because preliminary analyses indicated heterogeneity of variances among temperatures, which can be explicitly modeled within a GLS framework. To determine community-level shifts during the Coral Bleaching Automated Stress System, we performed a canonical analysis of principal coordinates (CAP) via the

‘ordinate’ function in ‘phyloseq’,¹⁵⁵ using Bray-Curtis dissimilarity to calculate distances.¹⁸⁰ We opted for a distance-based redundancy analysis because we had a priori hypotheses about the factors driving community dissimilarity patterns. CAP implements a multivariate multiple linear regression to maximize the fit between principal component coordinates and explanatory variables. To help identify the impact of each explanatory variable in driving patterns within ordination space, we ran a PERMANOVA with 999 permutations using the ‘adonis2’ command from the package ‘vegan’;¹⁵⁶ post-hoc pairwise comparisons were performed with the ‘pairwise.adonis2’ function and implemented Benjamini and Hochberg p-value corrections due to multiple comparisons.¹⁵⁷ To test the statistical significance of patterns of homogeneity of variance, we ran ‘betadisper’ with 999 permutations from the package ‘vegan,’ using Bray-Curtis distances.¹⁵⁶ We then ran an ANOVA on the ‘betadisper’ group dispersion results to determine if the variance of each group’s distance from the centroid was statistically significant. Post-hoc comparisons were performed with Tukey’s Honest Significant Differences test which corrects for multiple testing at a 95% confidence level.

To detect differentially abundant microorganisms within particular locations and/or treatments, we performed an indicator species analysis¹⁸¹ using the package ‘indicpecies’.¹⁵⁸ Here, we used the ‘multipatt’ command with 999 permutations and implemented the Benjamini and Hochberg p-value correction for multiple comparisons. Given we had multiple temperature treatments, we first sub-setted our phyloseq object to represent separate gulfs and mtORF lineages, and then ran ‘multipatt’ comparing Symbiodiniaceae communities across temperatures.

Prokaryotic community

For 16S reads, we used the R package ‘DADA2’ version 1.20¹⁵⁹ (<http://github.com/benjjneb/dada2>) to call amplicon sequence variants (ASVs). Here we used cutadapt in DADA2 to remove primer sequences.¹⁶⁰ We also assigned taxonomy using the SILVA 16S database release v138.1,¹⁸² specifically formatted for the classification of ASVs derived from ‘DADA2’¹³⁷ (<https://zenodo.org/records/4587955>). Using the R package ‘phyloseq’,¹⁵⁵ (<https://github.com/joey711/phyloseq>) we integrated ASVs, taxonomy, and sample information into a single object. We then removed all ASVs assigned to chloroplasts, mitochondria, eukaryotes, or unassigned at the kingdom level. We used the package ‘decontam’¹⁸³ to remove potential contaminants within ASV data, by implementing a statistical classification procedure on the basis of prevalence within our negative controls. We additionally removed singletons and performed an r-log transformation within the ‘DESeq2’ package¹⁶¹ prior to beta diversity analyses. Beta diversity analyses for 16S follow the same pipelines as for the ITS2 analyses described previously (e.g., CAP, homogeneity of variances, and indicator species analyses).

Physiological measurements

To determine the factors driving changes in chlorophyll *a* and host protein concentrations during the Coral Bleaching Automated Stress System (CBASS), we used nonlinear mixed effects models. Previous CBASS work has estimated thermal thresholds using Fv/Fm, which is a measure of photosynthetic efficiency. This has involved fitting separate log-logistic dose–response curves (DRCs) to each colony, from which an effective dose 50 (ED50) is calculated as the bleaching threshold and compared among sites for each species using one-way ANOVAs.¹⁸⁴ ED50 is the inflection point where Fv/Fm is 50% lower than the starting value. We wished to more comprehensively test and account for among-site effects, in order to better resolve differences in the functional form of the thermal response among regions and mtORFs. To achieve this, we modeled the thermal functional response curve incorporating fixed effects of region and mtORF, and random effects of site. Specifically, we modeled the thermal response of each physiological response variable as a logistic function of temperature:

$$y_{m,r,s}(x) = \frac{\nu_{m,r,s}}{1 + e^{(\delta_{m,r,s} \times (\log(x) - \log(\alpha_{m,r,s})))}} \quad (\text{Equation 1})$$

where $y_{m,r,s}(x)$ is the response of site *s*, within region *r*, and belonging to mtORF *m*, to temperature treatment *x*. Equation 1 has a sigmoid shape, declining from an asymptotic maximum value ν for the physiological response variable to a lower asymptote at zero. The parameter α is the temperature at which the physiological response has declined to 50% of that maximum value; we use this as our measure of threshold position – larger values of α imply that physiological condition is maintained at (i.e., more resistant to higher temperatures). The parameter δ regulates the steepness of this threshold, with larger values of δ implying steeper thresholds (i.e., the decline in performance from ν to zero is more concentrated around the threshold temperature α). For all parameters, our most general model allowed for differences depending on region *r* (upwelling or non-upwelling) and mtORF *m* (which we considered fixed effects of interest), and we also allowed random effects on the parameters of site within region. This allowed us to most effectively leverage the hierarchical structure in our data to resolve differences among regions and mtORFs. Although we initially also considered random effects on the parameters of colony within site, we removed these from our models to simplify the hierarchical structure of our data. This is because each colony has an associated mtORF lineage, and this was the most relevant source of colony-level differences. To fit our models to data, we used the ‘nlme’ package^{153,154} in the statistical program R version 4.2.1.¹⁶⁸

Specifically, for each response variable, we first fit a full model with an interaction between gulf and mtORF lineage as fixed effects on each parameter, and random effects of reef site within region and colony within site, on each of the three model parameters. We then systematically dropped fixed effects one at a time and compared model fits using likelihood ratio statistics to determine the best fixed-effects structure. We then repeated the same process to determine the random-effects structure. For all fixed-effects model selection fits, we used maximum likelihood (rather than Restricted Maximum Likelihood [REML]), to ensure comparability of likelihoods.¹⁸⁵ We also computed the Akaike information criterion (AIC) score for each of our fitted models, to determine whether the model selected by likelihood ratio tests was also the lowest AIC model.

Oxidative metabolism

To analyze the decline in LPO and TAC concentrations during the Coral Bleaching Automated Stress System (CBASS), we used linear mixed effects models. We built our models using ‘lm’ from the base ‘stats’ package in R version 4.2.1.¹⁶⁸ So that the response variables’ distributions approximated normal distributions, we log-transformed our LPO data and square-root transformed our TAC data. To explore if algal community dynamics could explain some of the variation in LPO and TAC during the CBASS, we additionally treated the relative proportion of the two algal clades (ratio of the relative reads mapping to *Cladocopium* spp. versus *Durisdinium* spp.) within each sample as an ordinal fixed effect.

As we had only three temperature treatments for our LPO data, we lacked the power to model this metric as a continuous function of temperature. Instead, we treated temperature as a categorical variable; as this approach can accommodate non-monotonic responses to temperature. We first created a full model where LPO was a function of temperature, region, mtORF, and algal clade ratio all as fixed effects. We also found support for an interactive effect between the fixed effects of region and mtORF lineage during our preliminary modeling, so this was additionally considered. We systematically removed fixed effects and compared nested model fits using the likelihood ratio test to determine the final fixed effects structure. We also calculated each model fit’s AIC score to confirm that the model selected on the basis of likelihood ratio tests was also the lowest AIC model. For TAC, we followed the same model selection process, with a few modifications. First, as we had four temperature treatments, we were able to model TAC as a continuous function of temperature. Previous work suggests that TAC’s responses to stress may be non-monotonic, as organisms may increase their TAC as stress increases from low levels but may decline at very high levels of stress as the organism’s capacity to cope with oxidative stress becomes overwhelmed.^{35,38} Therefore, we modeled TAC as a quadratic function of temperature, rather than a sigmoid function.